

## 7 Anhang

### 7.1 Summary

In this work HCl and DCI were examined with the help of the predissociationspectroscopy. For this UV-UV double resonance method a new experimental setup was realised using two nanosecond dye lasers. The first step of the experiment, the resonance enhanced multiphoton ionisation (REMPI), was realised utilizing one dye laser. The REMPI process offers thereby the possibility to prepare state selected HCl<sup>+</sup>- and DCI<sup>+</sup> ions, with which the angular momentum can be tuned. These state selected molecular ions represent promising precursors for investigations of ion molecule reactions. Further the spectroscopy of the HCl- and DCI  $f^3\Delta_2 \leftarrow X^1\Sigma^+$  transition is accessible by the REMPI step of the experiment. In the second part of the experiment the molecular ions are photoexcited into the  $A^2\Sigma^+$  state with the help of the second laser system. Due to the fact, that the  $A^2\Sigma^+$  state can predissociate, one receives the predissociation spectra (PD-spectra) of the HCl<sup>+</sup>- and DCI<sup>+</sup>  $A^2\Sigma^+ \leftarrow X^2\Pi_{3/2}$  transitions. The photodissociation causes formation of Cl<sup>+</sup> ions, which can be detected using a time of flight mass spectrometer. Via the PD-spectra it was possible to determine the rotational state distribution of the DCI<sup>+</sup>/HCl<sup>+</sup> ions formed in the REMPI step. In addition, the spectroscopic parameters of the HCl<sup>+</sup>- and DCI<sup>+</sup>  $A^2\Sigma^+$ -states have been derived. Finally, through the analysis of the linewidth and lineprofile conclusions on the predissociationdynamics of HCl<sup>+</sup> and DCI<sup>+</sup> can be drawn. In particular, this yields in the exact determination of the predissociationthreshold.

New spectroscopic parameters  $\nu_0$ , B, D and H for the HCl and DCI  $f^3\Delta_2(v''=0)$  Rydberg state were achieved from the  $f^3\Delta_2 \leftarrow X^1\Sigma$  REMPI spectra. So far, according to knowledge on available literature, this is the first time that these parameters for H<sup>37</sup>Cl and D<sup>37</sup>Cl were determined.

The PD spectra of the HCl<sup>+</sup>  $A^2\Sigma^+(v' = 4-6) \leftarrow X^2\Pi_{3/2}(v'' = 0)$ - and DCI<sup>+</sup>  $A^2\Sigma^+(v' = 6-9) \leftarrow X^2\Pi_{3/2}(v'' = 0)$  transitions result from a one color (1+1) photodissociation, whereas

the resonant states are below the predissociation threshold. As a result, the spectroscopic parameters of these states can be determined. Data from literature on emission spectroscopy experiments compares well with the  $\text{DCI}^+$  states, but not with the  $\text{HCl}^+$  states, observed in this study.

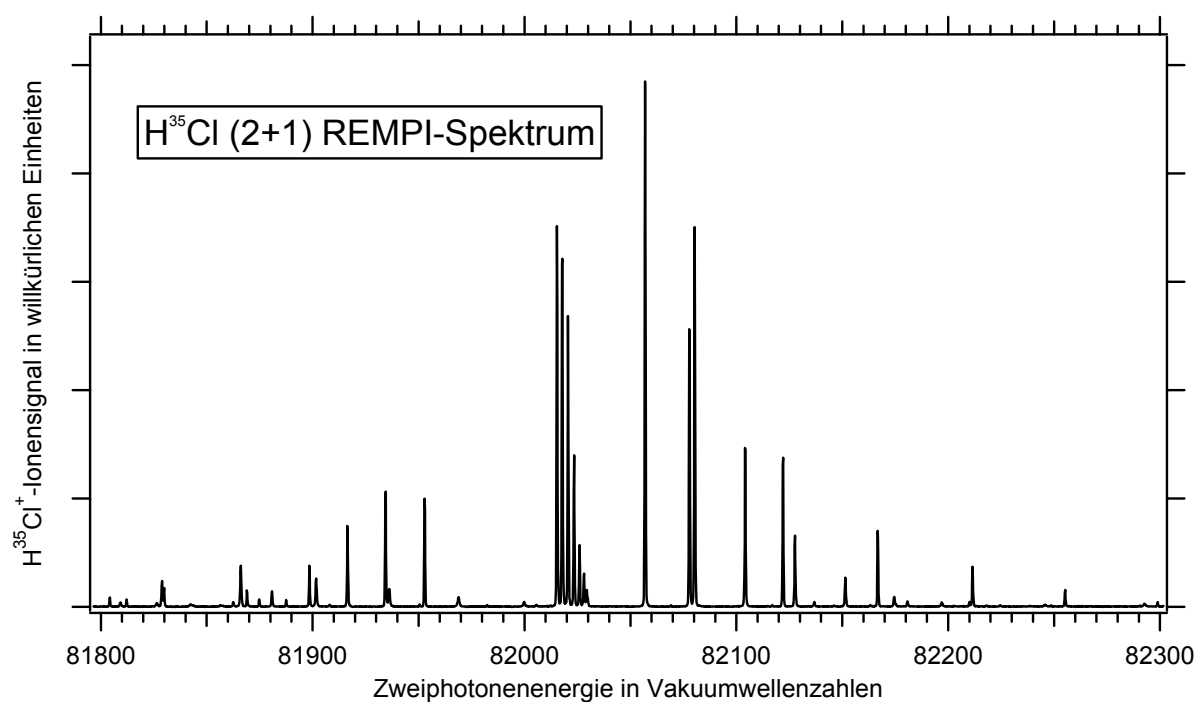
For the  $\text{HCl}^+ A^2\Sigma^+(v' = 7)$ - as well as the  $\text{DCI}^+ A^2\Sigma^+(v' = 10)$  state the rotational constants  $B$ , the  $\gamma$ -coupling constants and the transition energy  $T_v$  have been determined. Data for  $B$  and  $\gamma$  of these states were previously not available, since no rotational resolved spectra were accessible. From the  $\text{HCl}^+ A^2\Sigma^+(v' = 7)$ - and the  $\text{DCI}^+ A^2\Sigma^+(v' = 10)$  PD-spectra one derives the rotational state distribution of the ions formed via different pump lines in the REMPI process. It could be shown that the ionisation via the  $f^3\Delta_2(v''=0)$  Rydberg state leads to a high rotational state selectivity and a narrow rotational state distribution of the ions in the  $X^2\Pi_{3/2}$  state. Ions are formed in not more than four different rotational states, whereat about 70% of all ions are formed in just two rotational states. By proper choice of the pump line (tuning from R(1) to R(2)) in the REMPI spectrum the distribution in the  $\text{HCl}^+/\text{DCI}^+ X^2\Pi_{3/2}$  state can be shifted from  $N'' = 0-1$  to  $N'' = 4-5$ . A line profile analysis of a step in the  $\text{HCl}^+ A^2\Sigma^+(v' = 7)$  spectrum gave a new value for the dissociation energy of  $D_0(\text{HCl}^+) = 37536,7 \pm 0,5 \text{ cm}^{-1}$ . Combining this value with literature data on the ionisation energy of HCl and Cl, a new value for the dissociation energy of the neutral HCl have been derived as  $D_0(\text{HCl}) = 35747,2 \pm 1,2 \text{ cm}^{-1}$ .

Therefore in this work the predissociation spectra of the  $\text{HCl}^+ A^2\Sigma^+(v' = 8-10) \leftarrow \text{HCl}^+ X^2\Pi_{1/2}(v'' = 0)$ - as well as the  $\text{DCI}^+ A^2\Sigma^+(v' = 11,12) \leftarrow \text{DCI}^+ X^2\Pi_{1/2}(v'' = 0)$  transitions were obtained. For these states the predissociation lifetime as a function of the vibrational quantum number is observed. Within the  $\text{HCl}^+$  states the shortest lifetime of  $\tau = 0.063(12) \text{ ps}$  was determined in the  $(v' = 8)$  state. For higher vibrational quantum numbers the predissociation lifetime increases again. This experimental finding shows a similar trend, as already available theoretical work.

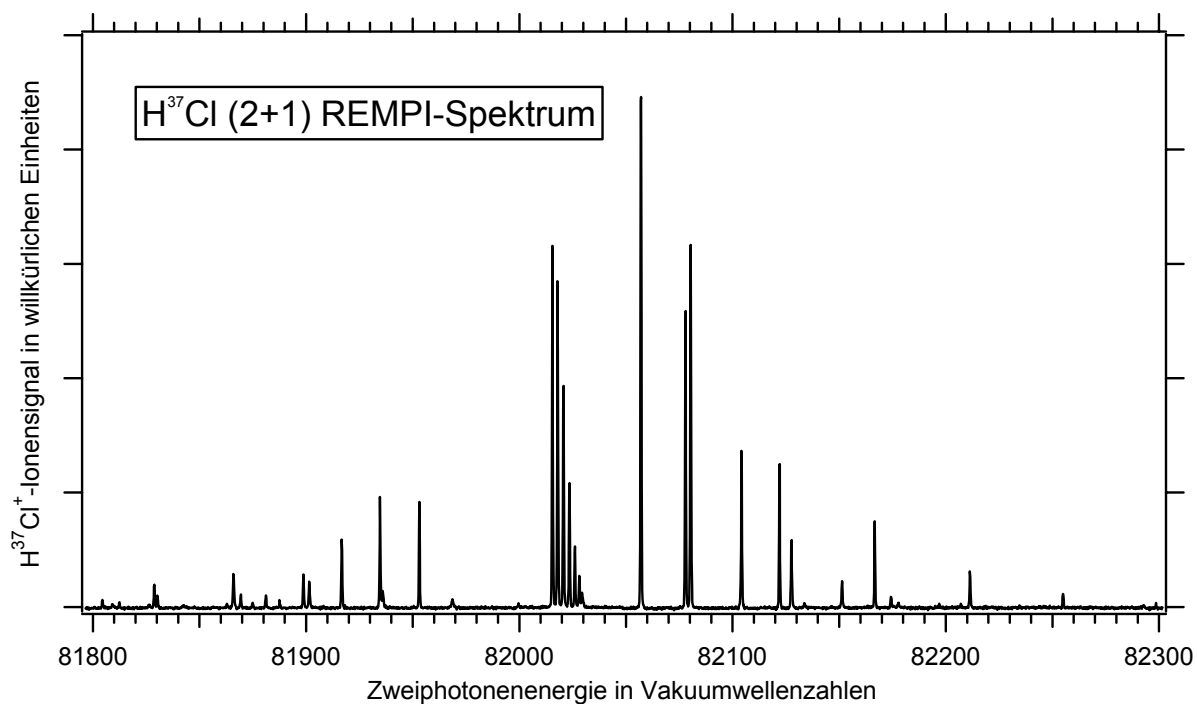
## 7.2 Spektrenverzeichnis

In diesem Abschnitt sind die REMPI-Spektren über den  $f^3\Delta_2$ -Zustand sowie die PD-Spektren der  $A^2\Sigma^+ \leftarrow X^2\Pi_{3/2}$  Übergänge, die im Rahmen dieser Arbeit aufgenommen wurden, zusammengestellt.

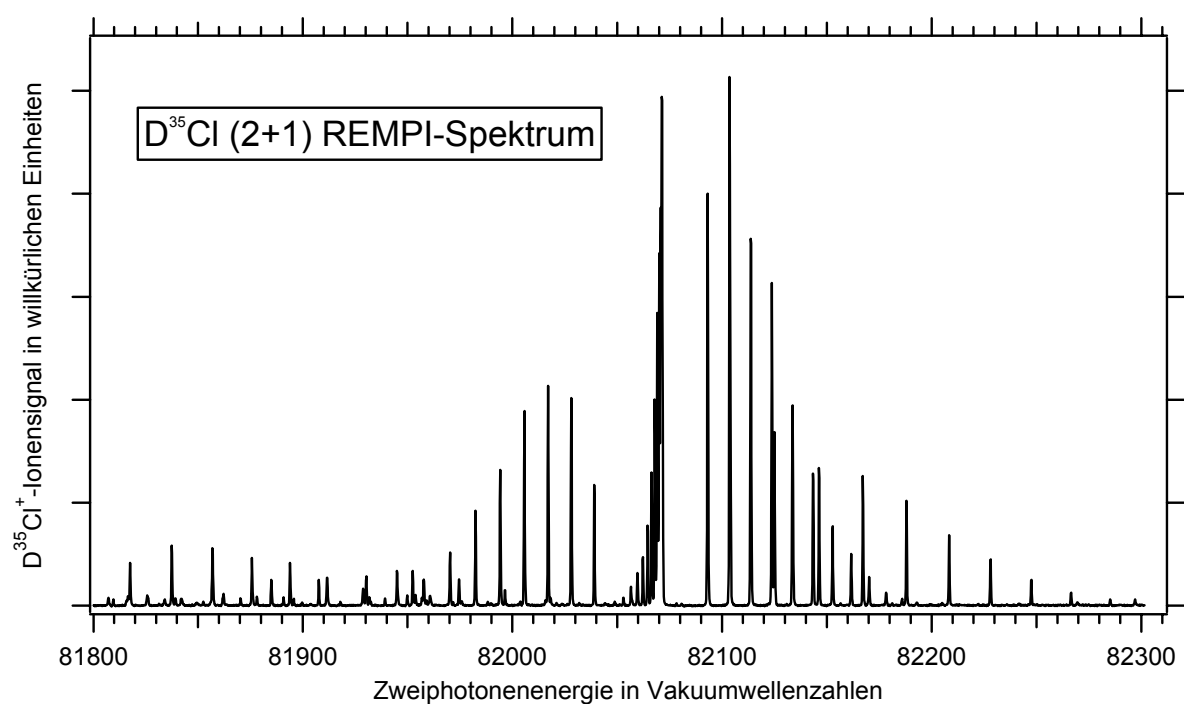
### 7.2.1 REMPI-Spektren über den $f^3\Delta_2$ -Zustand



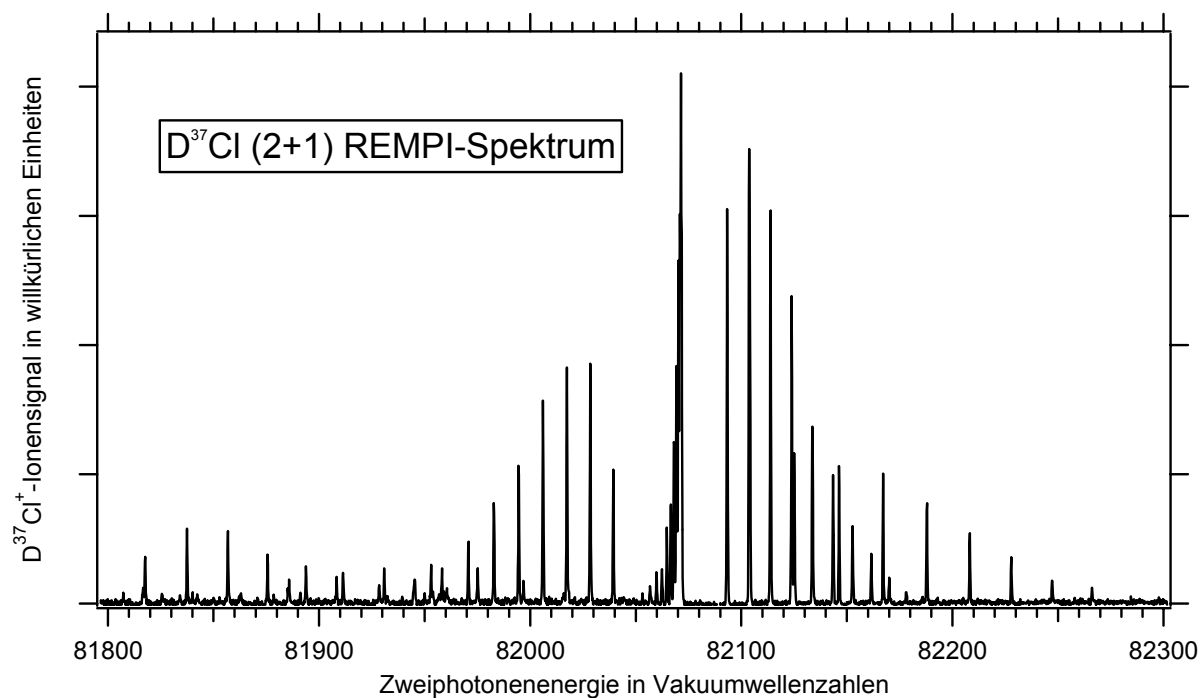
(2+1) REMPI-Spektrum über den  $H^{35}Cl f^3\Delta_2 \leftarrow X^1\Sigma^+$ -Übergang.



(2+1) REMPI-Spektrum über den  $\text{H}^{37}\text{Cl } f^3\Delta_2 \leftarrow X^1\Sigma^+$ -Übergang.

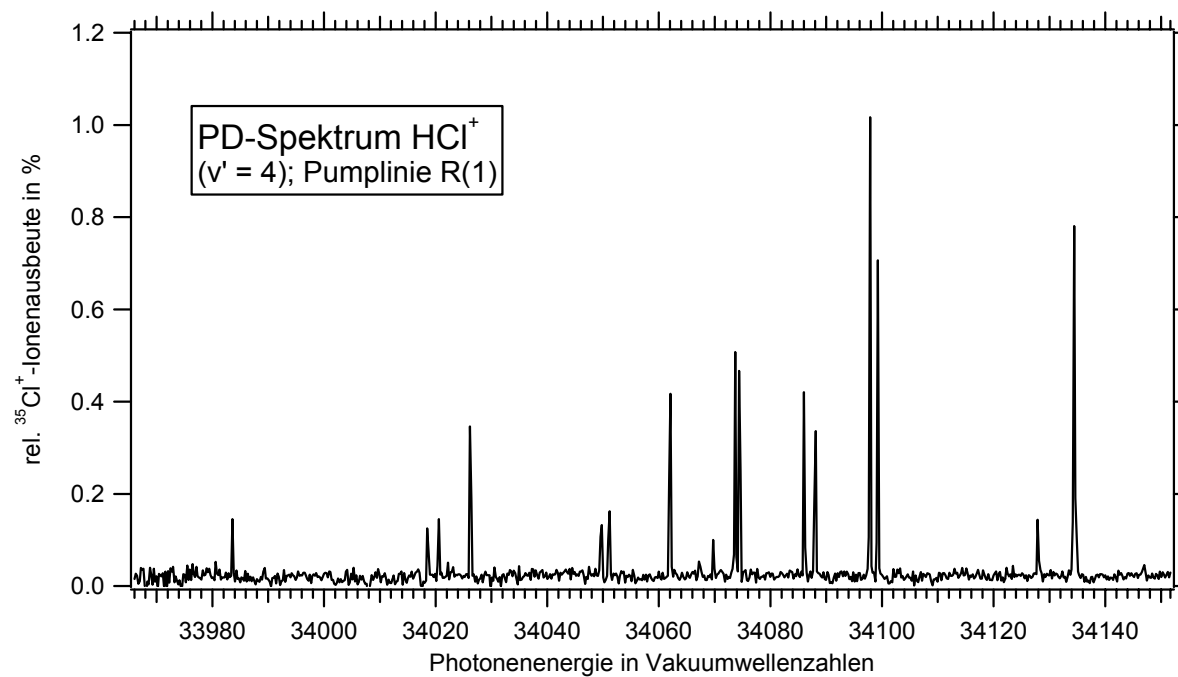


(2+1) REMPI-Spektrum über den  $\text{D}^{35}\text{Cl } f^3\Delta_2 \leftarrow X^1\Sigma^+$ -Übergang.

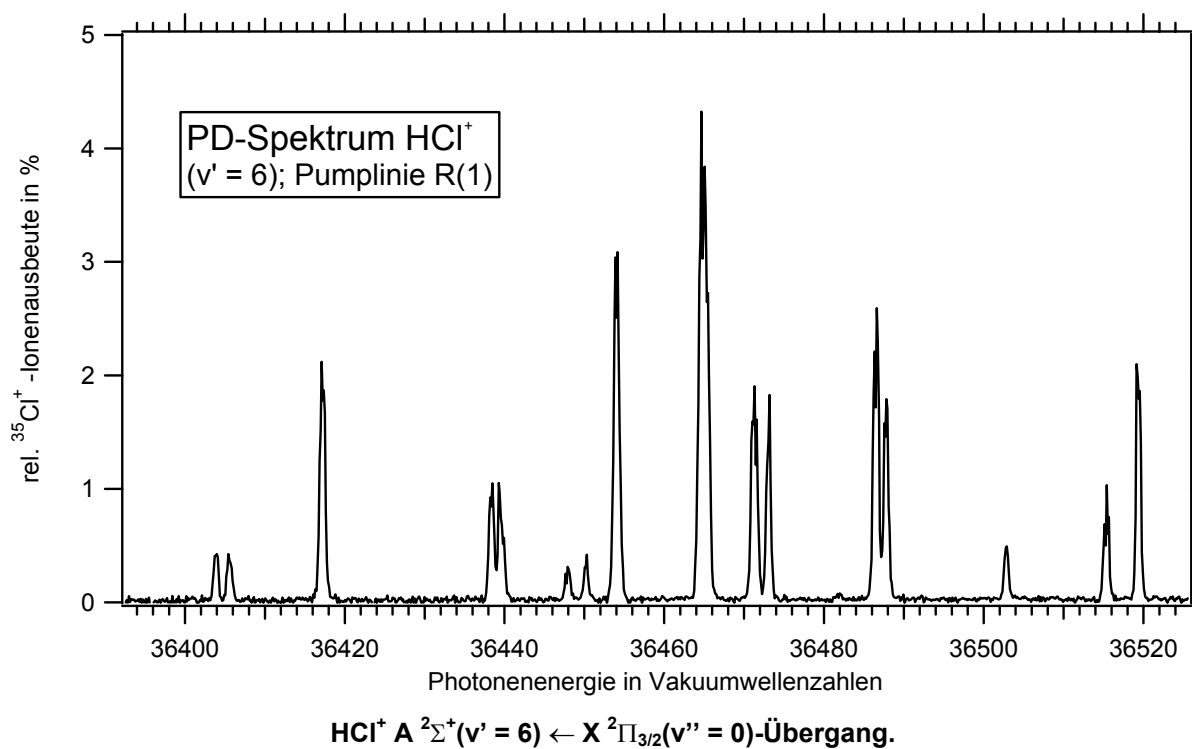
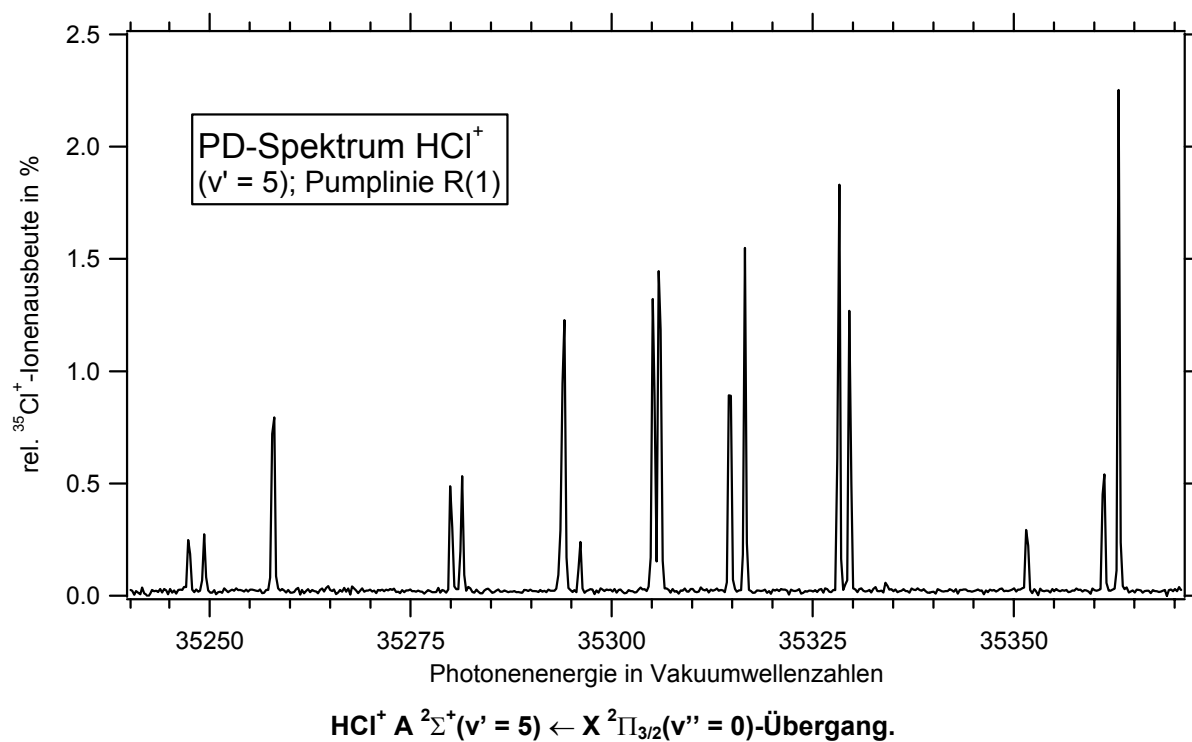


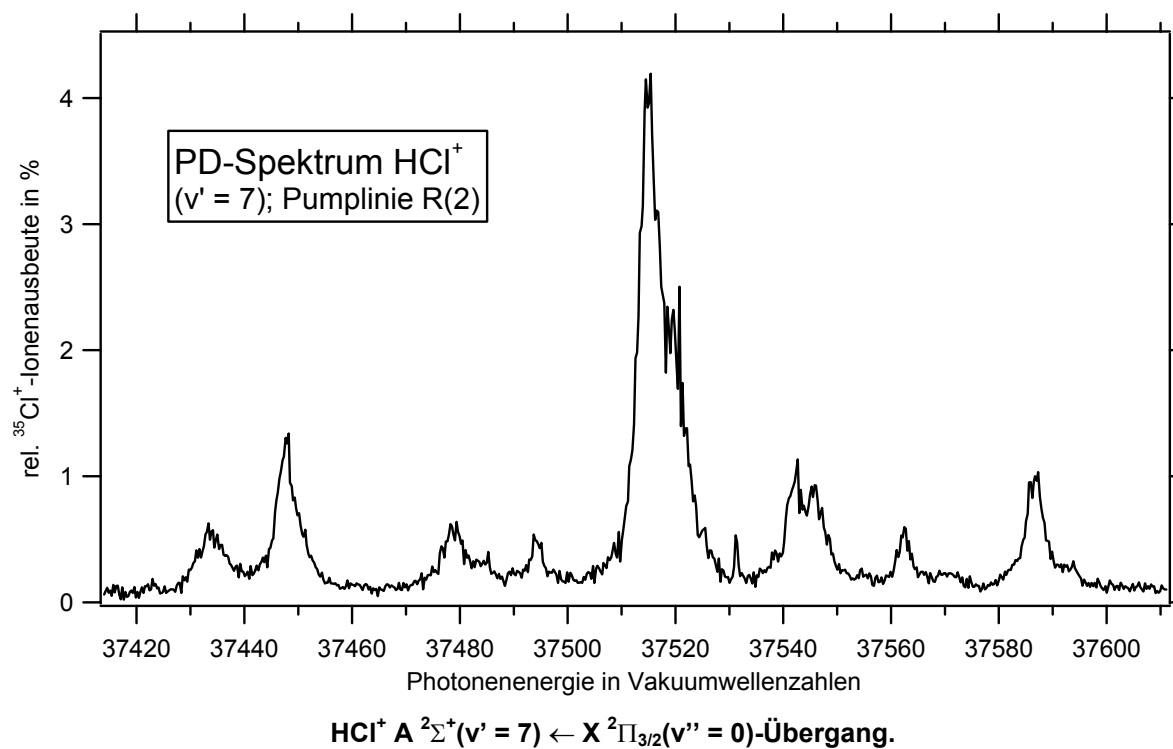
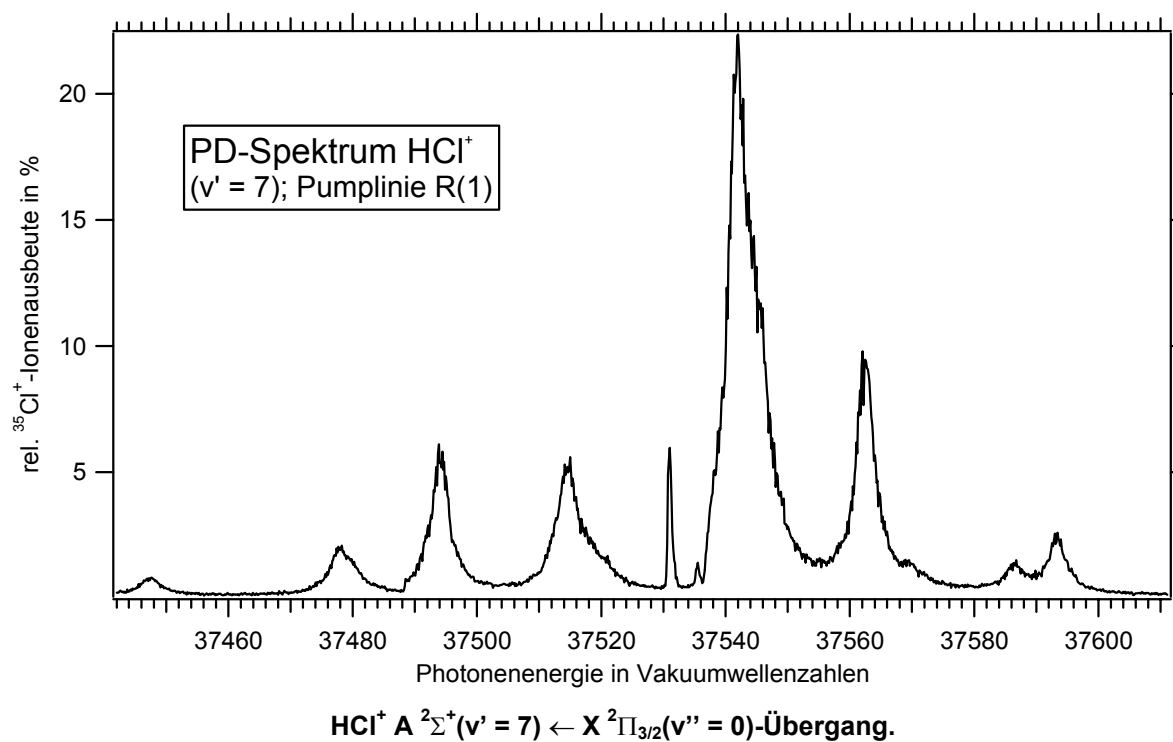
$(2+1)$  REMPI-Spektrum über den  $D^{37}\text{Cl } f^3\Delta_2 \leftarrow X^1\Sigma^+$ -Übergang.

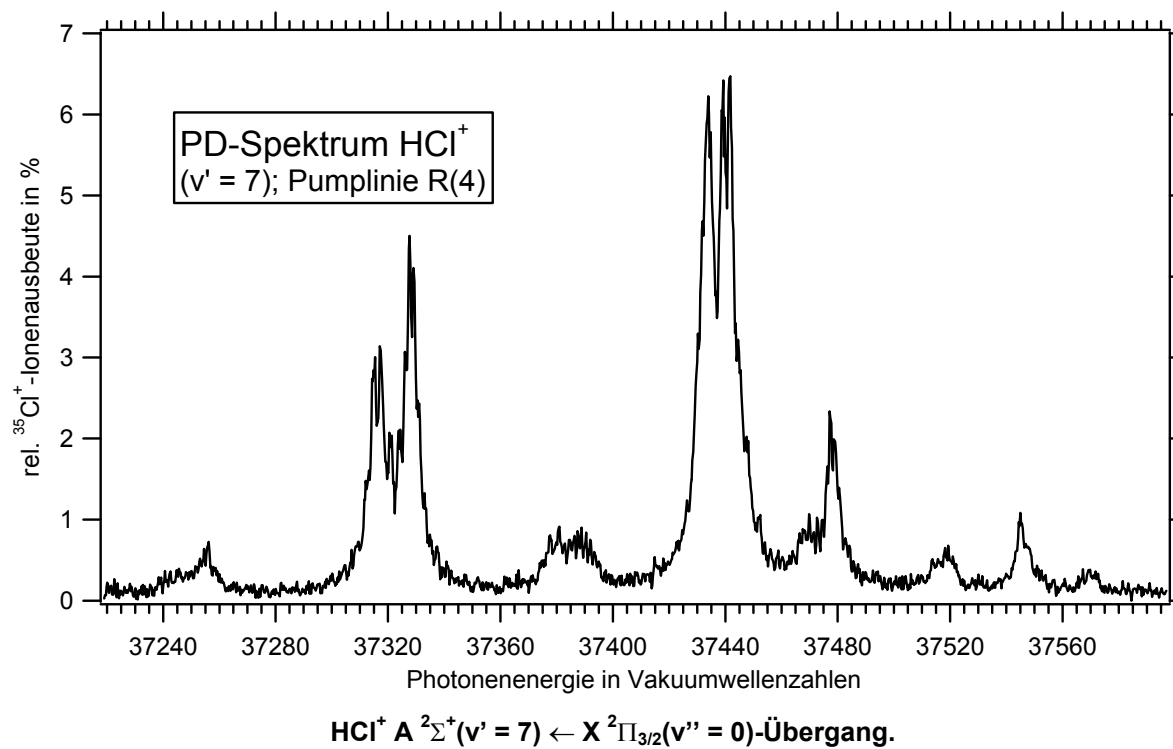
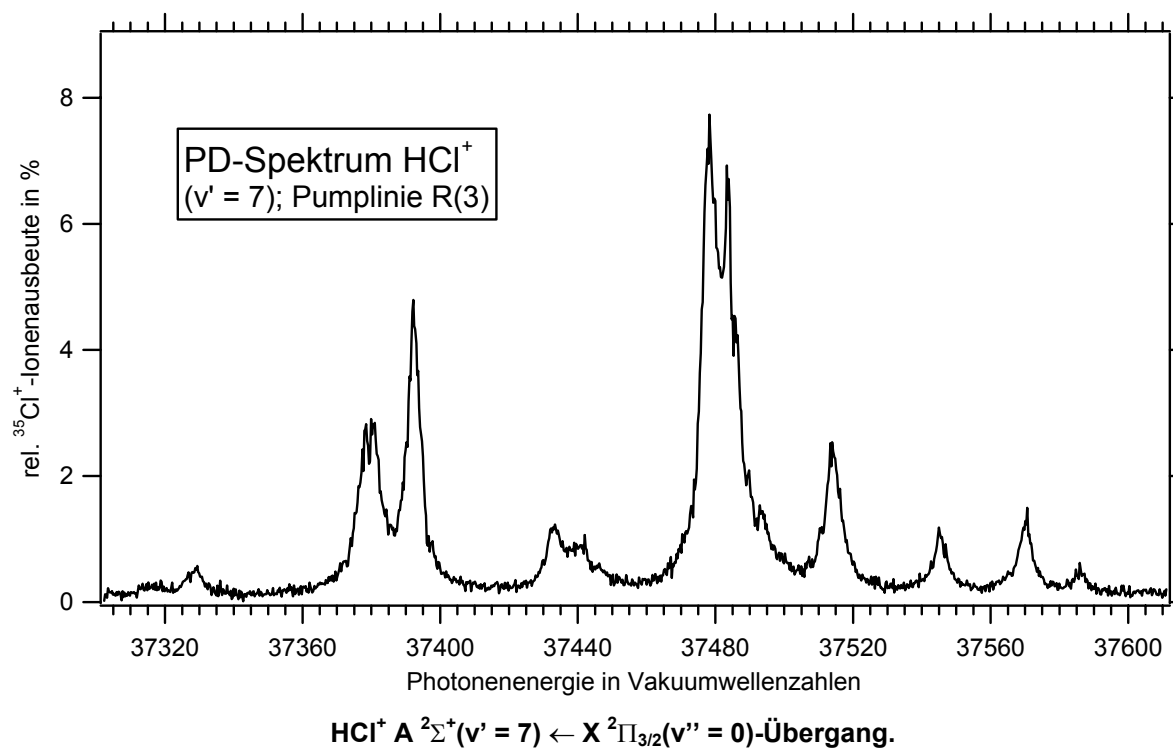
### 7.2.2 PD-Spektren der $\text{HCl}^+ A^2\Sigma^+ \leftarrow X^2\Pi_{3/2}$ -Übergänge



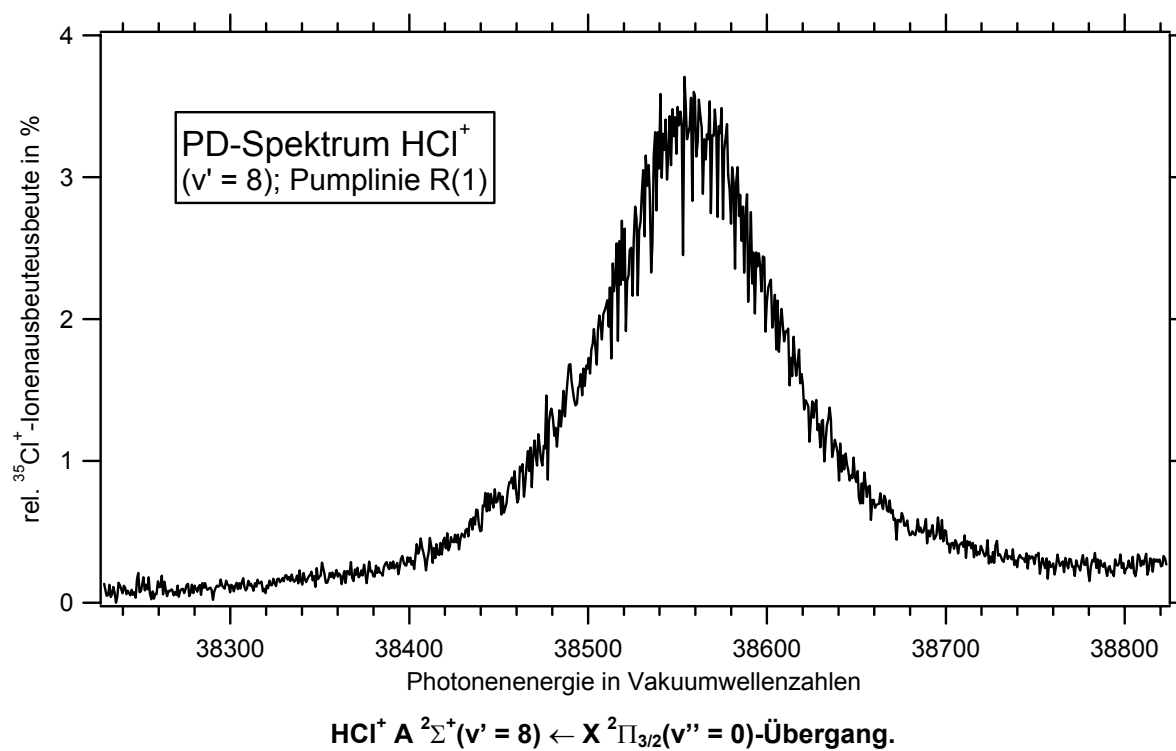
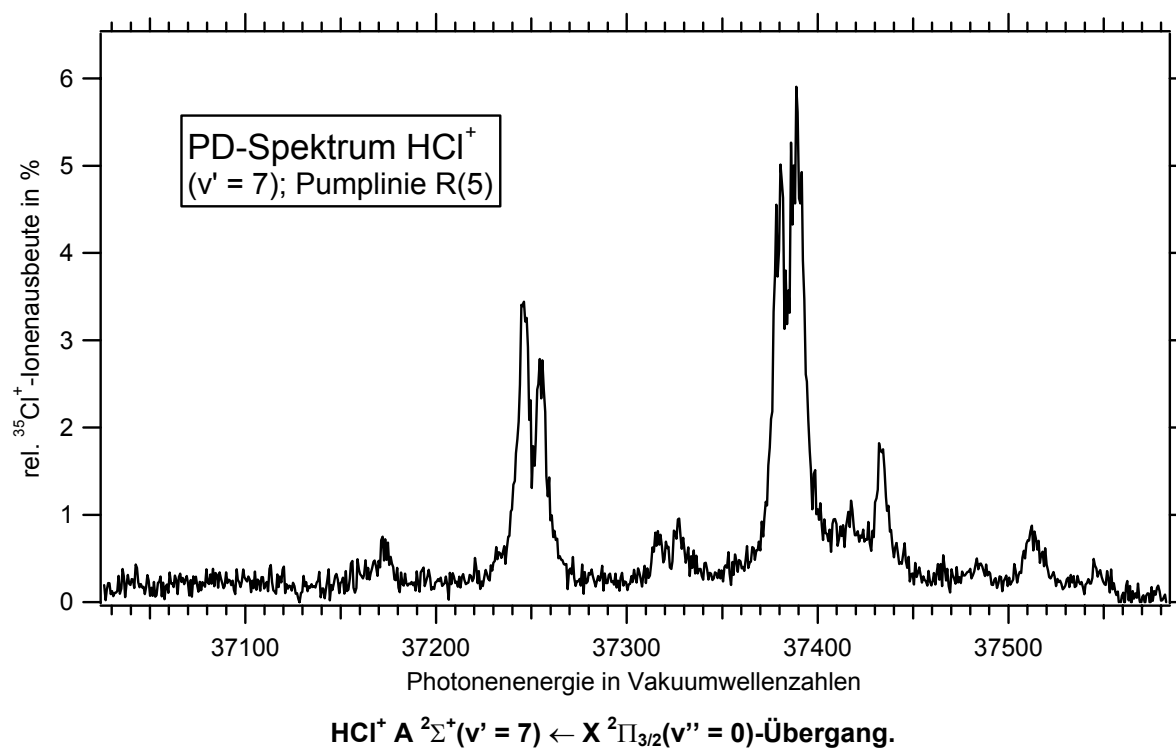
$\text{HCl}^+ A^2\Sigma^+(v' = 4) \leftarrow X^2\Pi_{3/2}(v'' = 0)$ -Übergang.

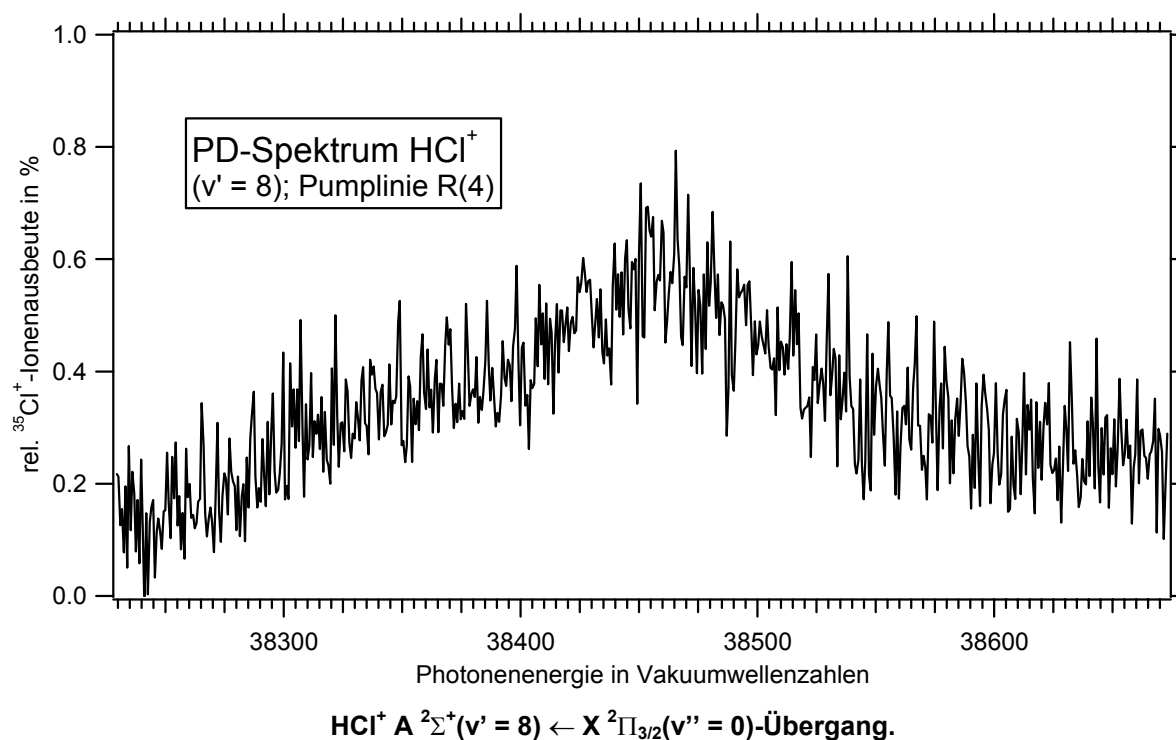
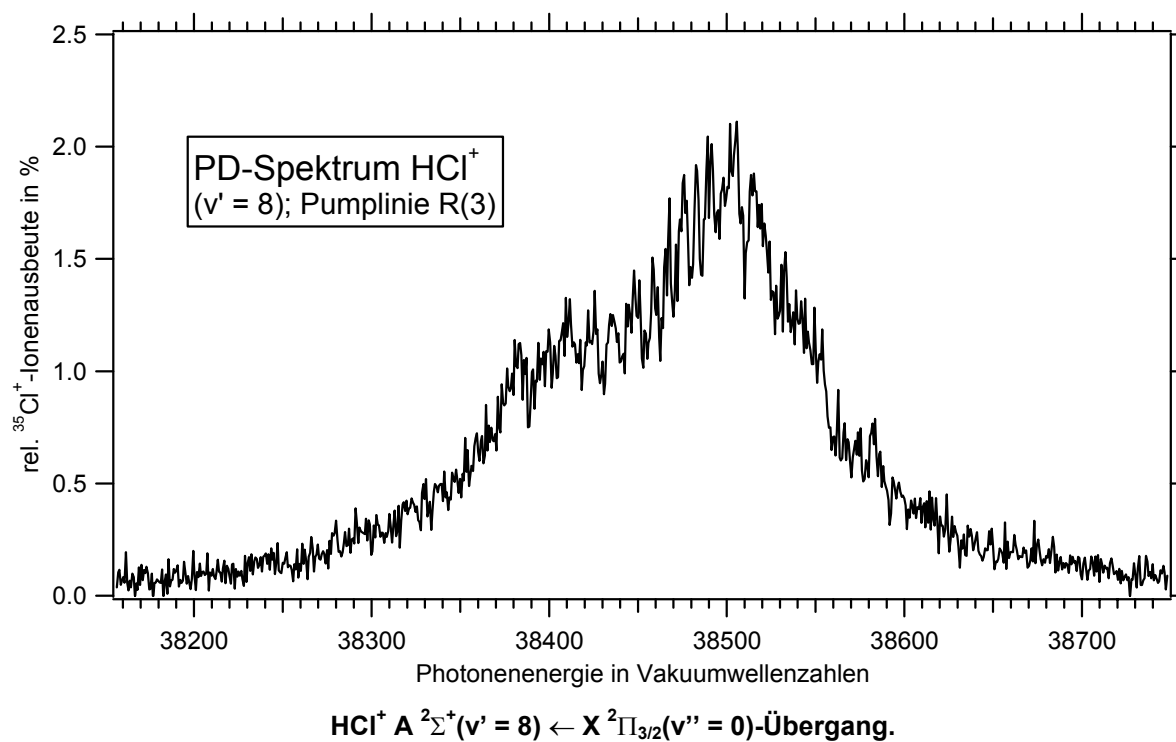


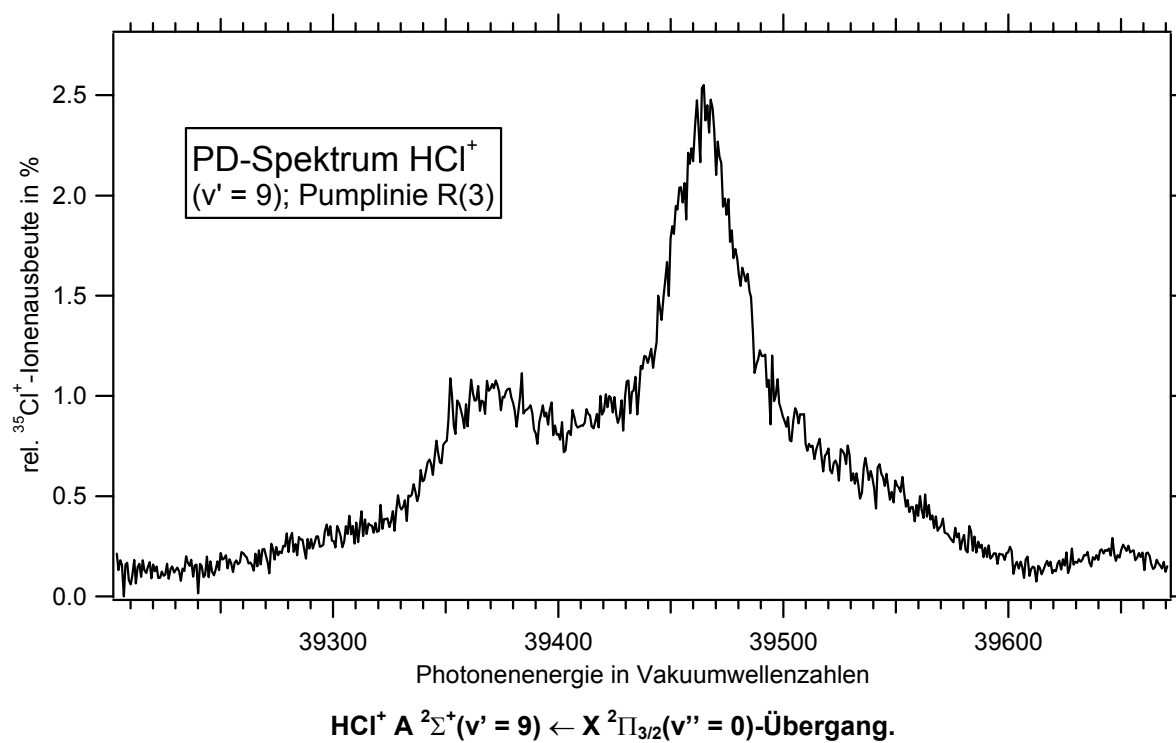
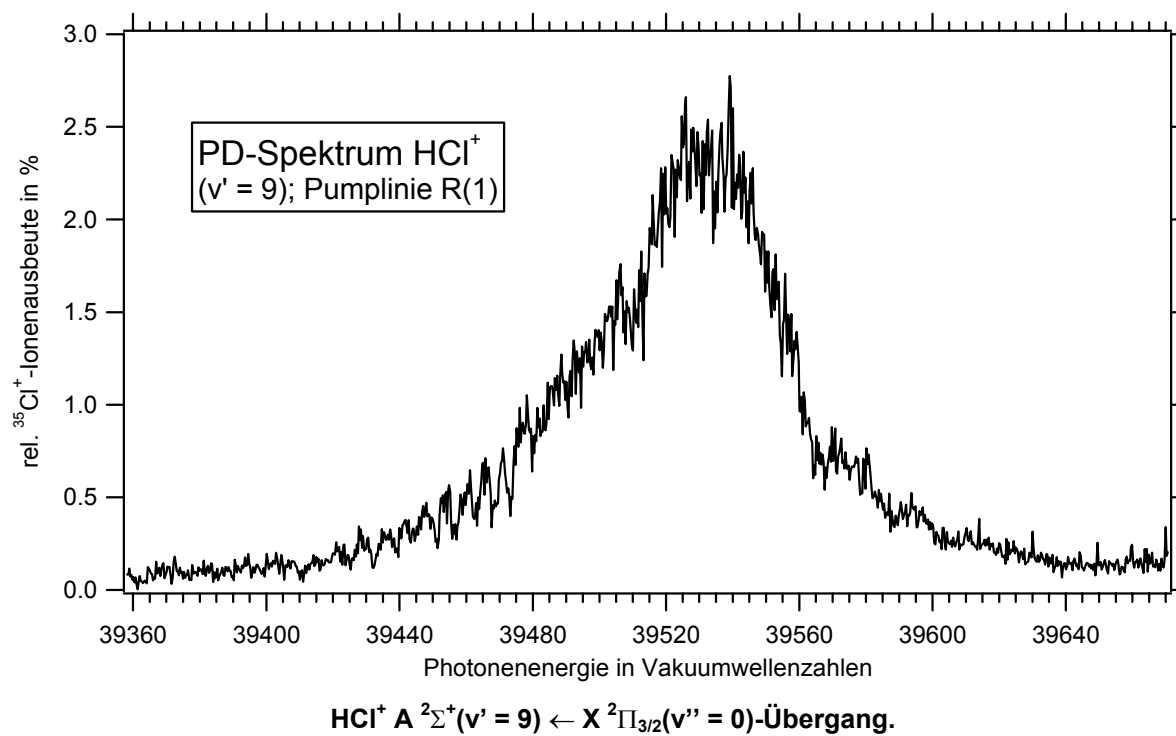


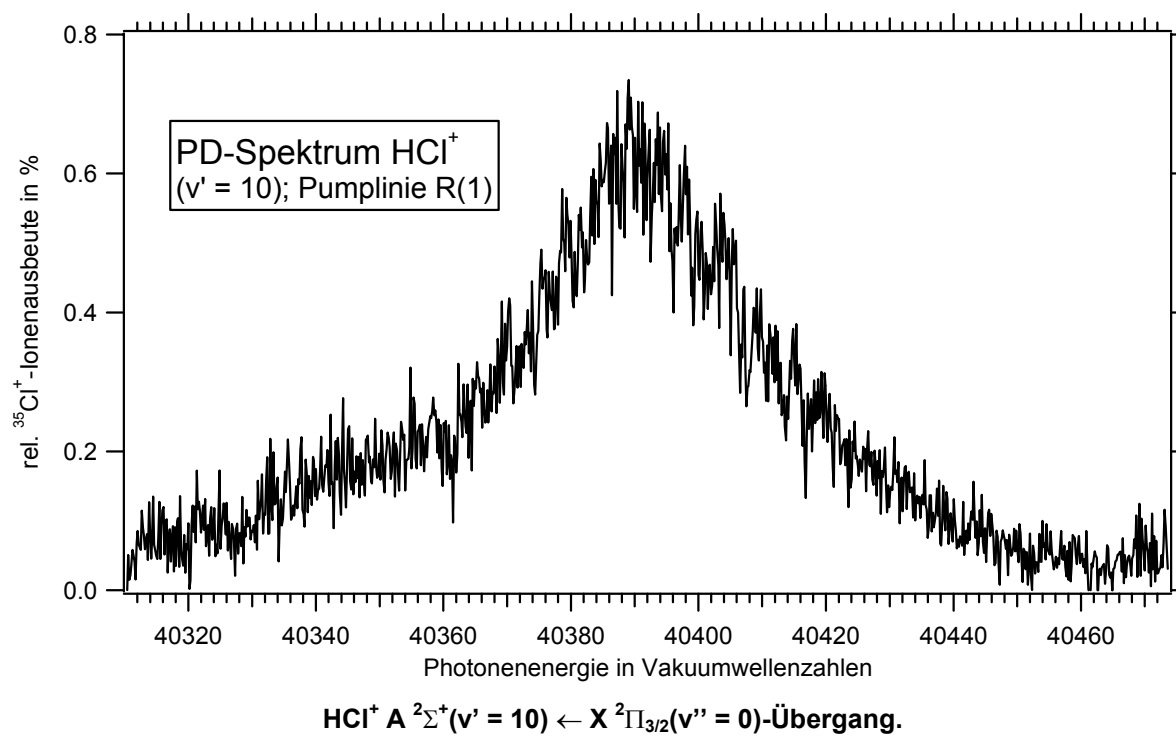
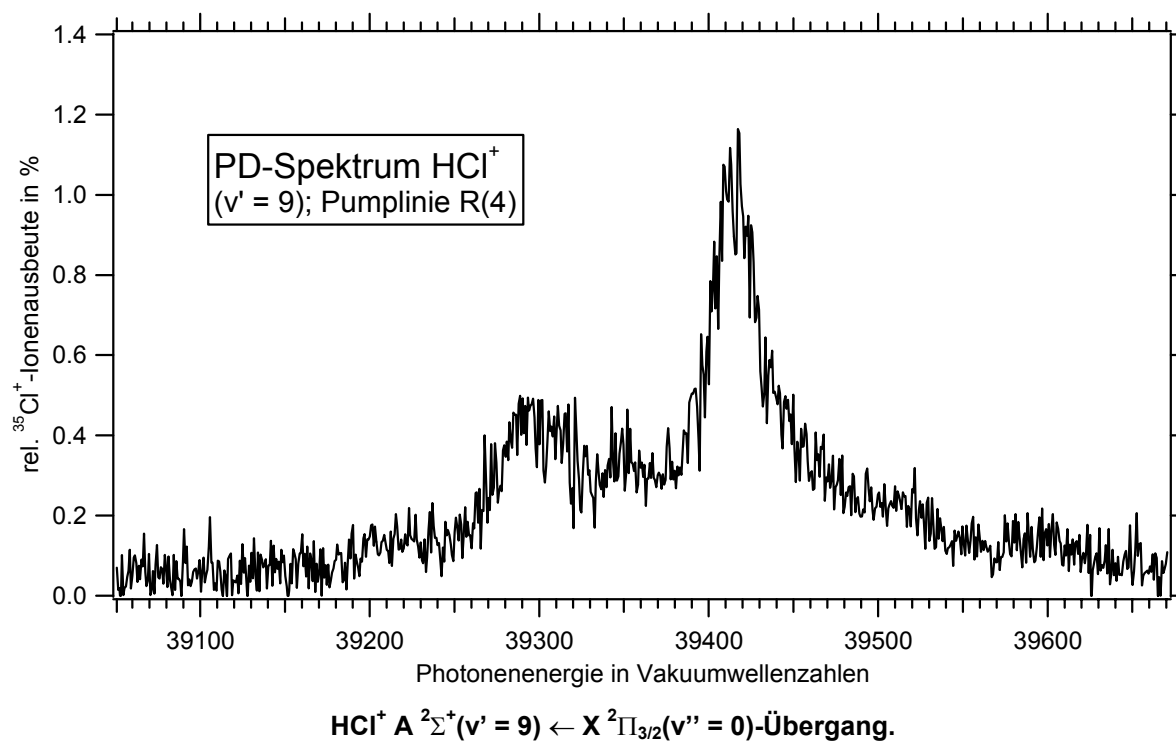


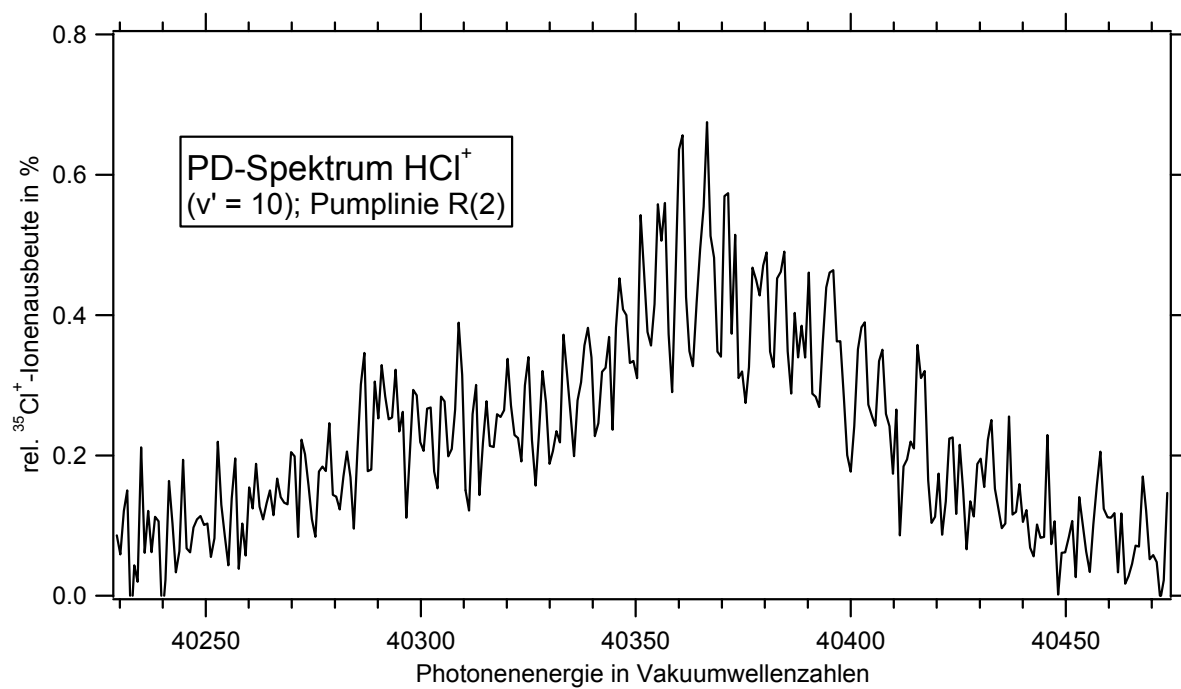




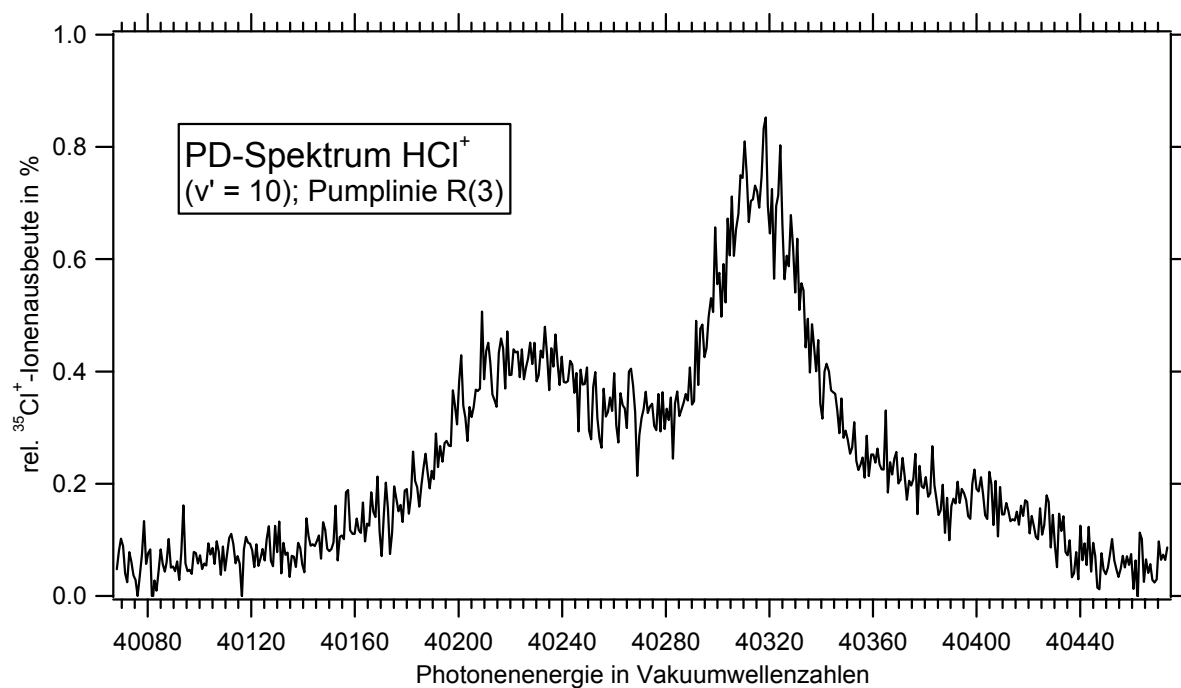




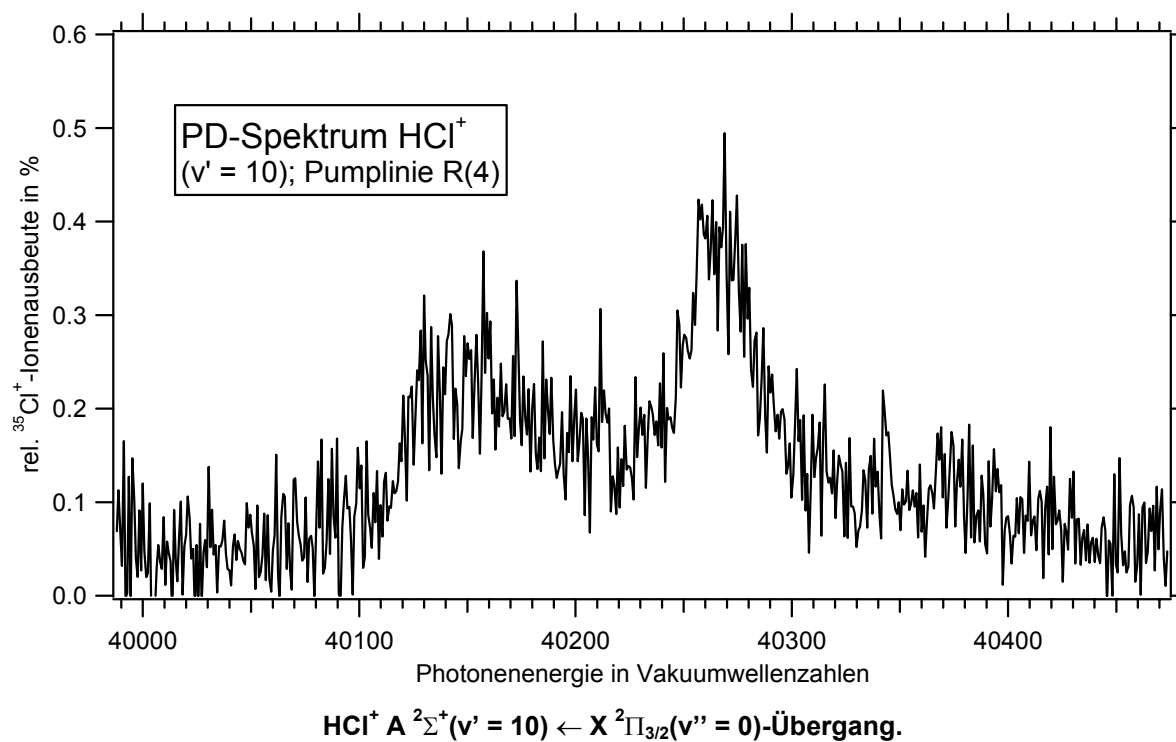




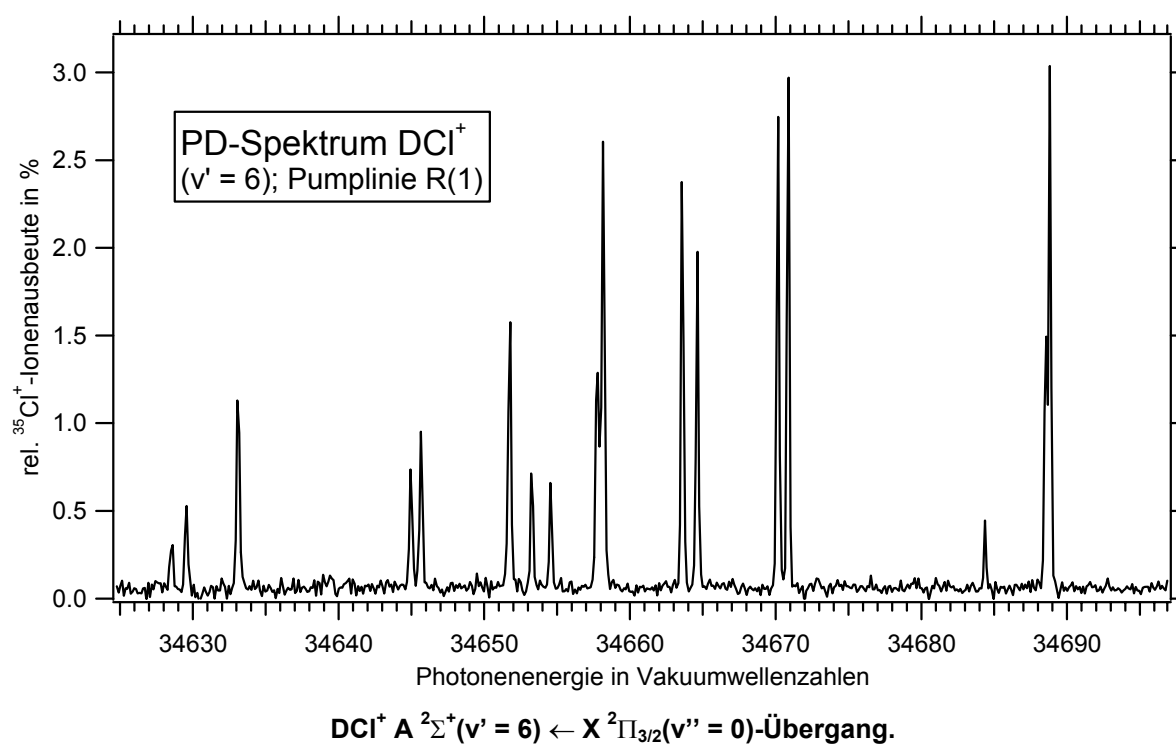
$\text{HCl}^+ \text{ A } ^2\Sigma^+(v' = 10) \leftarrow \text{X } ^2\Pi_{3/2}(v'' = 0)$ -Übergang.

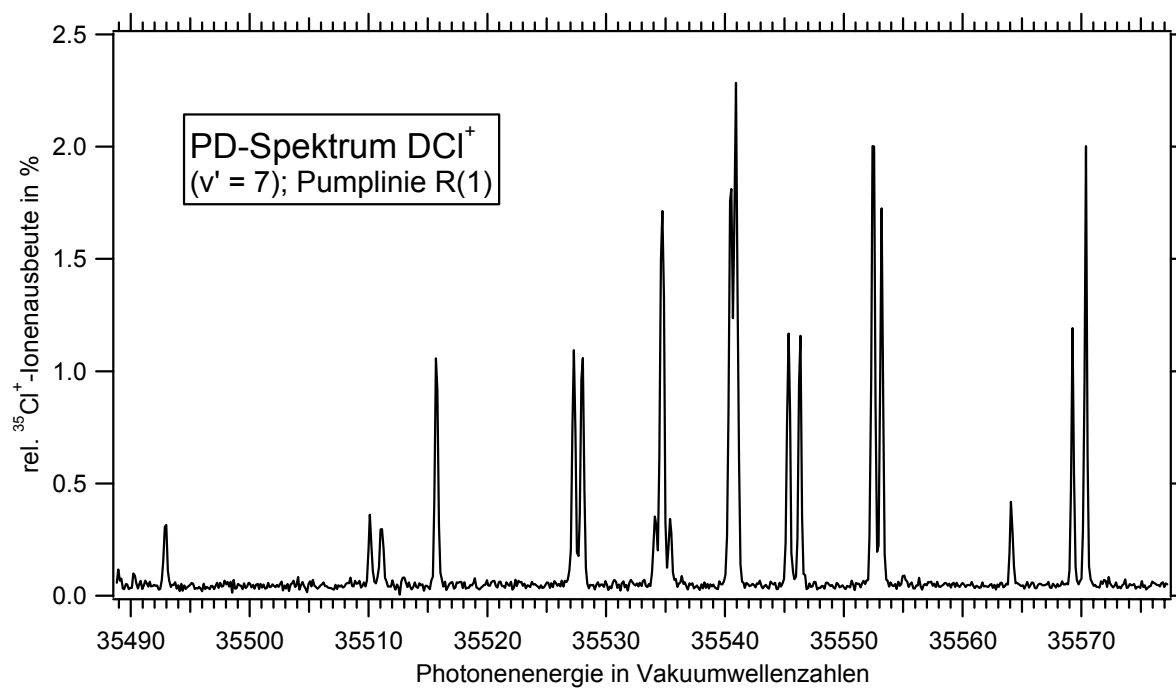


$\text{HCl}^+ \text{ A } ^2\Sigma^+(v' = 10) \leftarrow \text{X } ^2\Pi_{3/2}(v'' = 0)$ -Übergang.

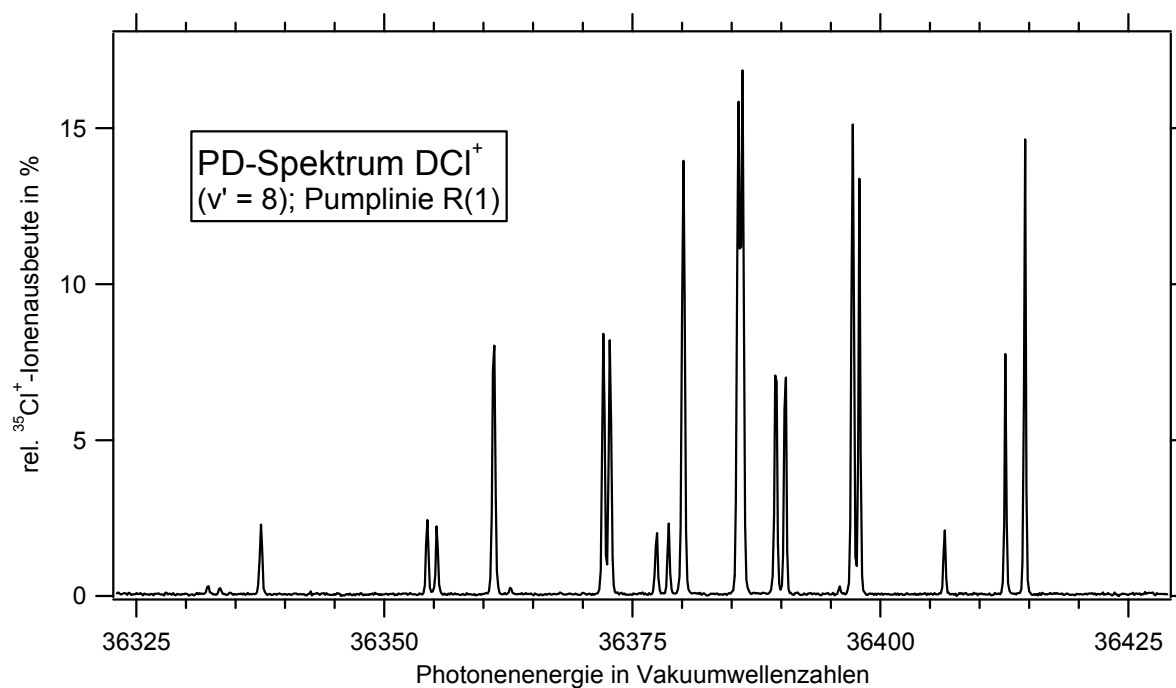


### 7.2.3 PD-Spektren der $\text{DCI}^+ \text{ A } ^2\Sigma^+ \leftarrow \text{X } ^2\Pi_{3/2}$ -Übergänge

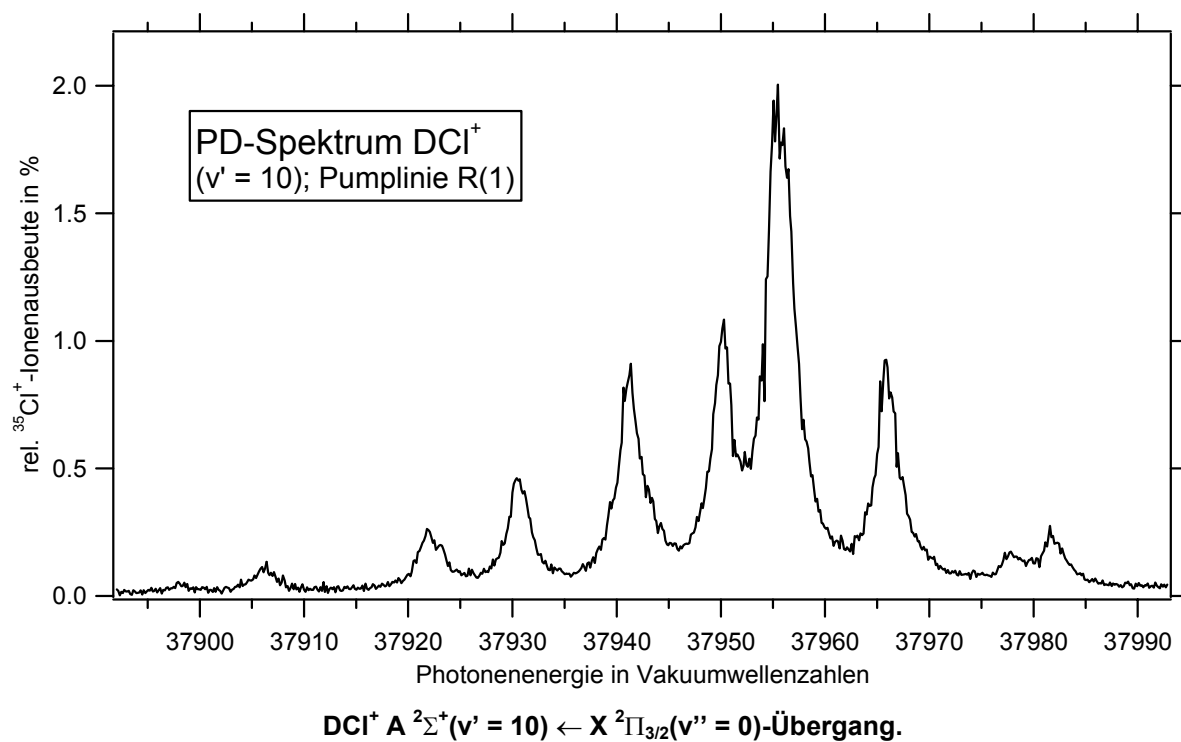
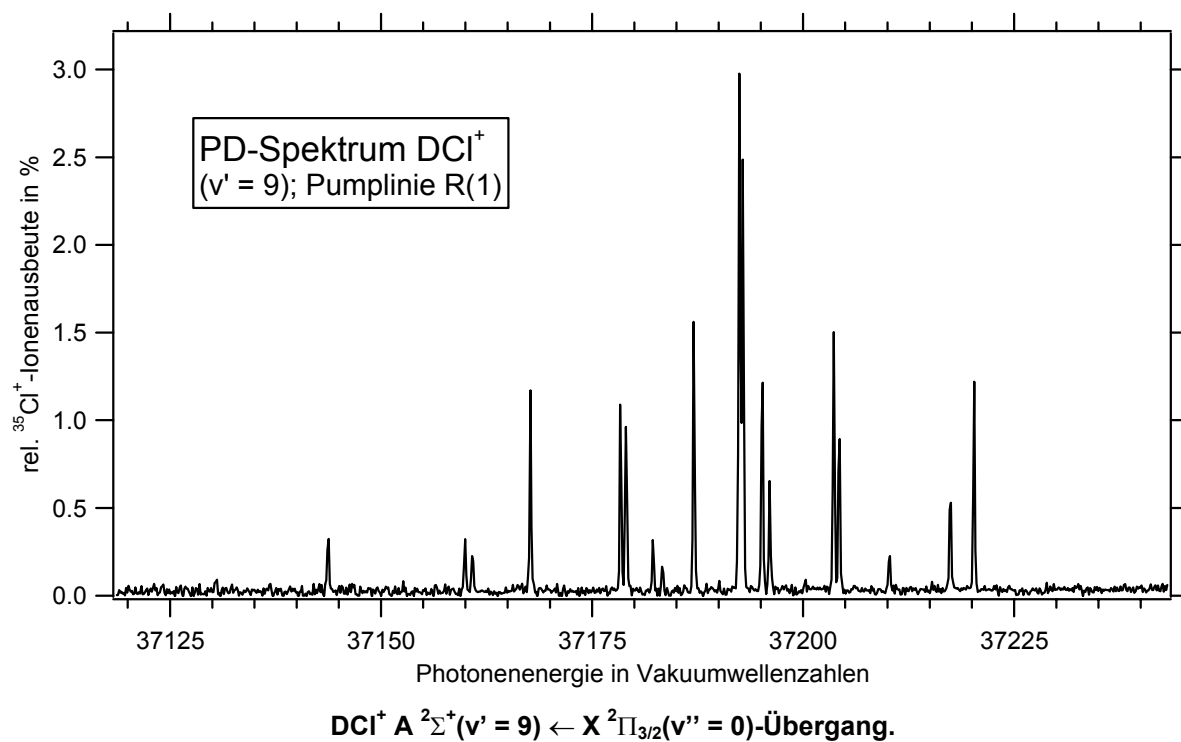




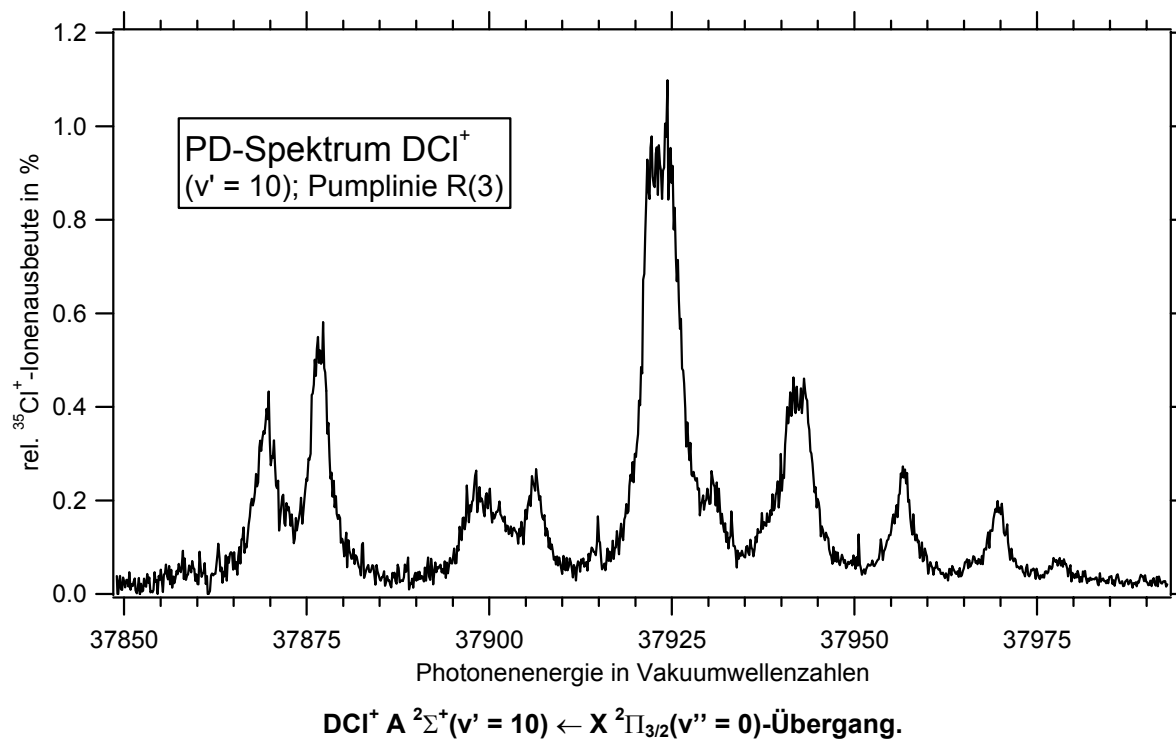
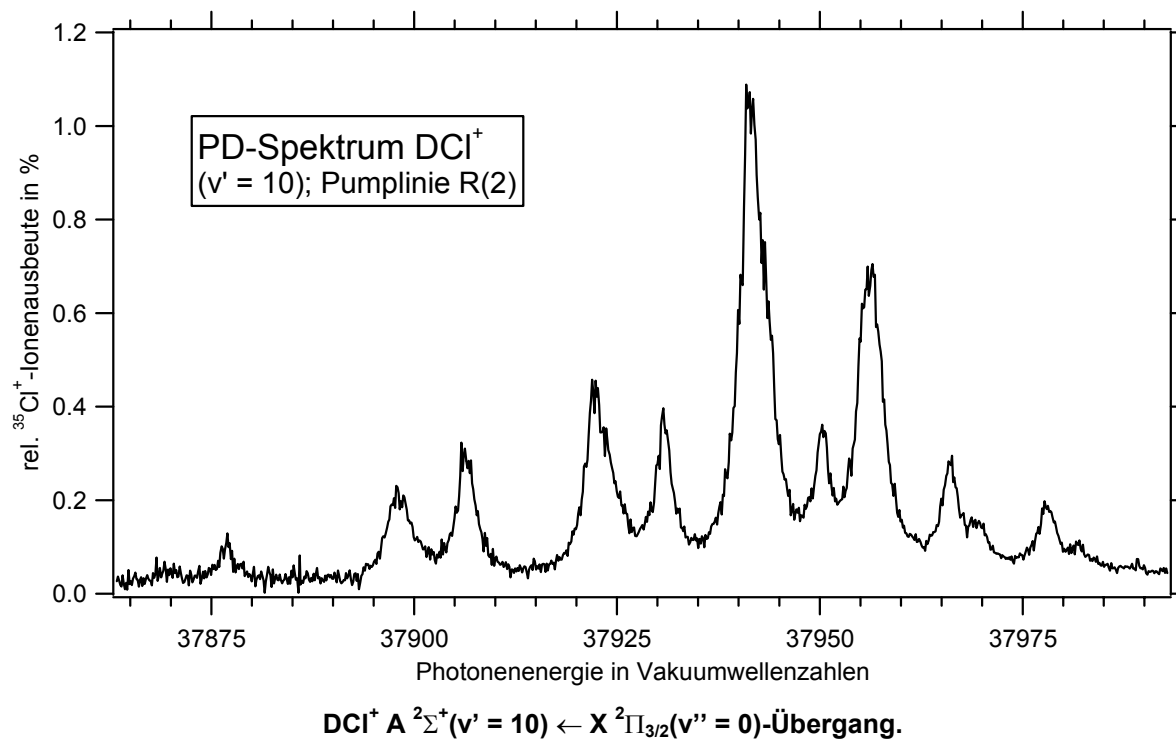
$\text{DCI}^+ \text{A } ^2\Sigma^+(v' = 7) \leftarrow \text{X } ^2\Pi_{3/2}(v'' = 0)$ -Übergang.

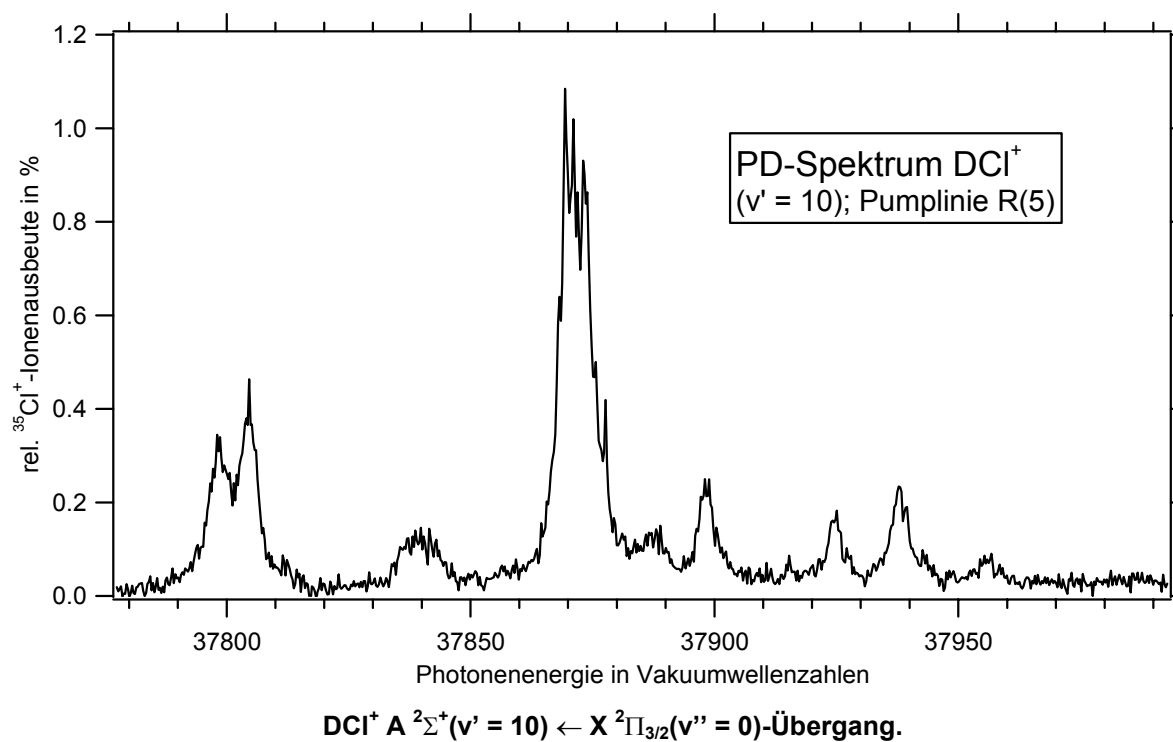
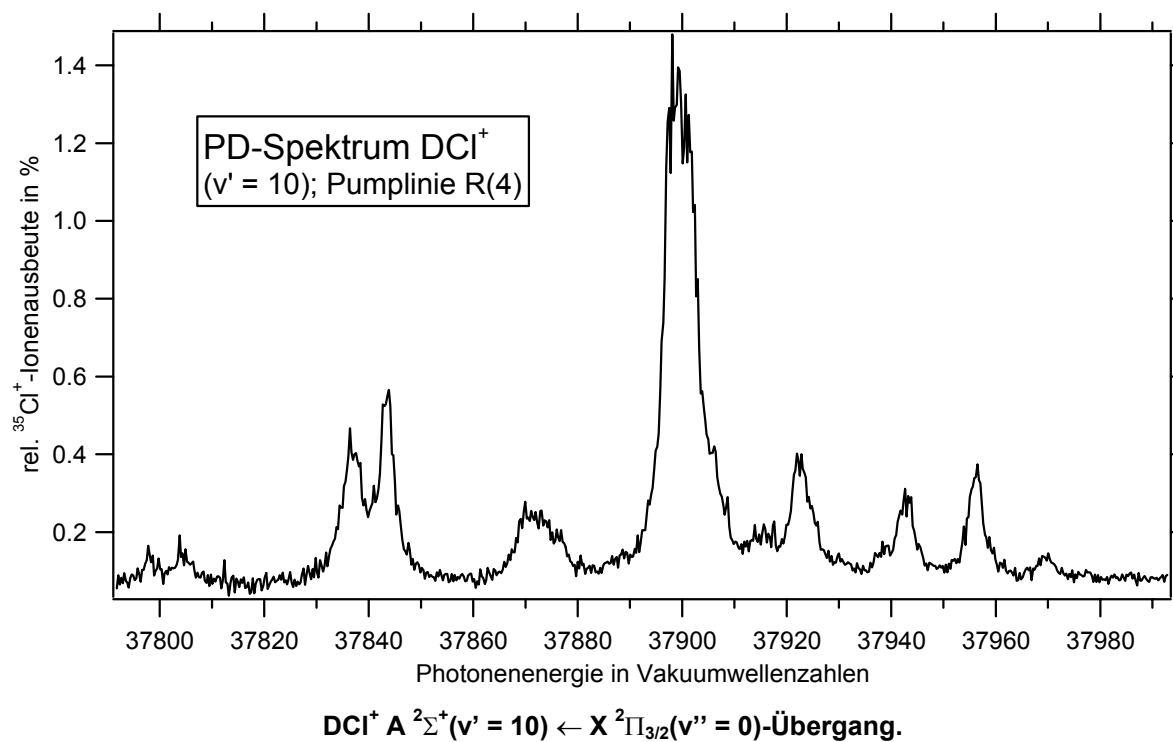


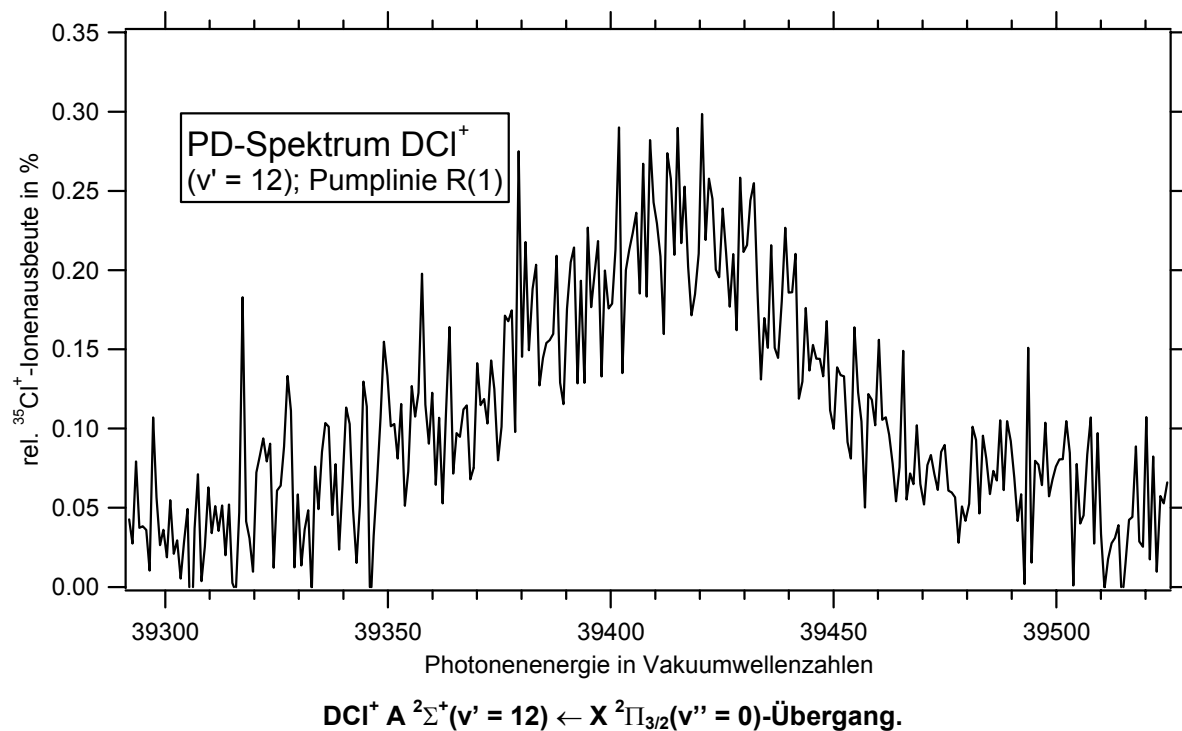
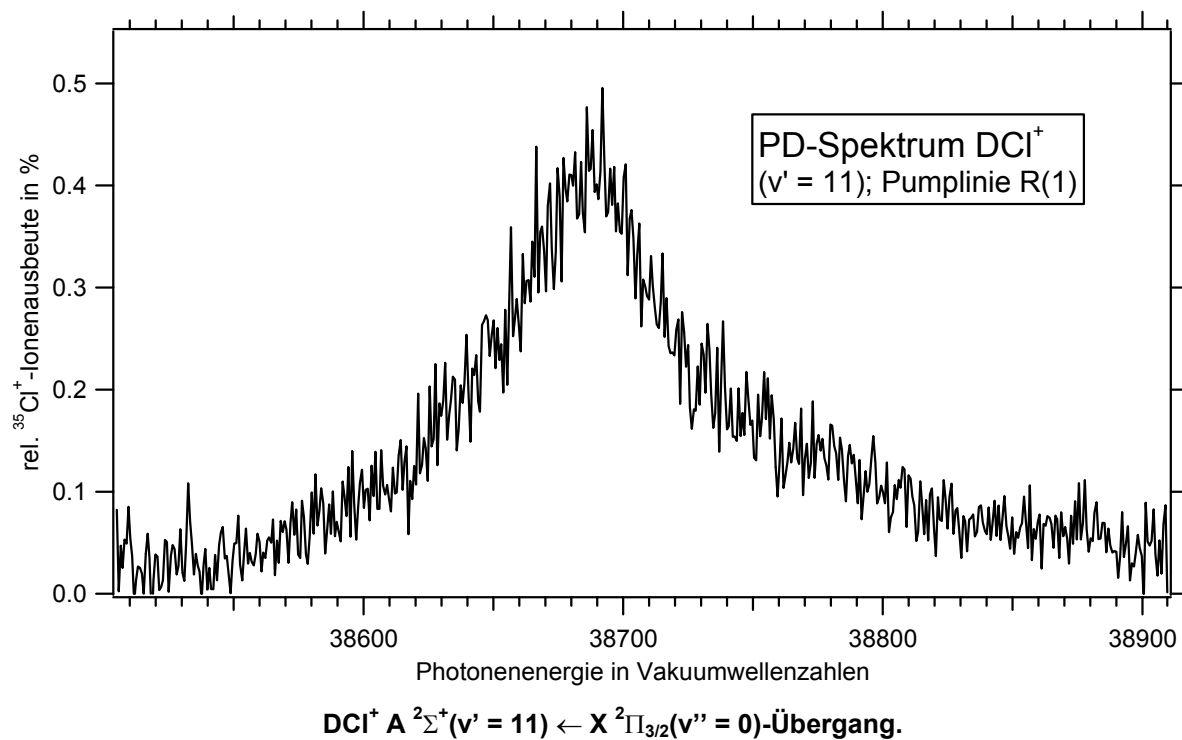
$\text{DCI}^+ \text{A } ^2\Sigma^+(v' = 8) \leftarrow \text{X } ^2\Pi_{3/2}(v'' = 0)$ -Übergang.











## 7.3 Übergangsintensitäten und Franck-Condon Faktoren

Nachfolgend sind die Übergangsintensitäten  $S(J'', J')$  sowie die Franck-Condon Faktoren, die für die Berechnung der theoretischen  $\text{HCl}^+ A^2\Sigma^+(v' = 7-10)$ - bzw.  $\text{DCI}^+ A^2\Sigma^+(v' = 10-12)$ -Spektren herangezogen wurden, aufgelistet.

### Übergangsintensitäten für $\text{HCl}^+ A^2\Sigma^+ \leftarrow \text{HCl}^+ X^2\Pi$ -Übergänge:

Zweig	$P_1$	$Q_{21}$	$R_1$	$P_{21}$	$Q_1$	$R_{21}$
$J'' = 1.5$	0.514	0.377	0.109	0.485	0.424	0.091
$J'' = 2.5$	0.635	0.626	0.24	0.564	0.746	0.19
$J'' = 3.5$	0.776	0.841	0.383	0.651	1.064	0.285
$J'' = 4.5$	0.929	1.036	0.535	0.735	1.388	0.377
$J'' = 5.5$	1.090	1.214	0.695	0.815	1.723	0.462
$J'' = 6.5$	1.260	1.377	0.863	0.889	2.070	0.541
$J'' = 7.5$	1.436	1.525	1.038	0.957	2.428	0.615
$J'' = 8.5$	1.620	1.661	1.220	1.019	2.799	0.683

### Übergangsintensitäten für $\text{DCI}^+ A^2\Sigma^+ \leftarrow \text{DCI}^+ X^2\Pi$ -Übergänge:

Zweig	$P_1$	$Q_{21}$	$R_1$	$P_{21}$	$Q_1$	$R_{21}$
$J'' = 1.5$	0.508	0.388	0.105	0.492	0.412	0.095
$J'' = 2.5$	0.618	0.654	0.228	0.581	0.717	0.201
$J'' = 3.5$	0.747	0.894	0.359	0.681	1.011	0.308
$J'' = 4.5$	0.884	1.119	0.497	0.782	1.305	0.413
$J'' = 5.5$	1.027	1.334	0.639	0.881	1.604	0.516
$J'' = 6.5$	1.175	1.539	0.786	0.977	1.908	0.615
$J'' = 7.5$	1.327	1.735	0.938	1.071	2.218	0.711
$J'' = 8.5$	1.484	1.924	1.093	1.161	2.535	0.804
$J'' = 9.5$	1.644	2.104	1.252	1.248	2.859	0.894
$J'' = 10.5$	1.808	2.277	1.415	1.331	3.189	0.980
$J'' = 11.5$	1.976	2.443	1.582	1.411	3.526	1.062
$J'' = 12.5$	2.147	2.602	1.752	1.488	3.870	1.142
$J'' = 13.5$	2.322	2.753	1.926	1.562	4.221	1.218
$J'' = 14.5$	2.500	2.898	2.103	1.632	4.518	1.291

### Franck-Condon Faktoren für $\text{HCl}^+ \text{A } ^2\Sigma^+ \leftarrow \text{HCl}^+ \text{X } ^2\Pi_{3/2}$ -Übergänge:

$\text{HCl}^+ \text{A } ^2\Sigma^+(v' = 7, N') \leftarrow \text{HCl}^+ \text{X } ^2\Pi_{3/2}(v'' = 0, N'')$									
$N'$	$N'' = 0$	$N'$	$N'' = 1$	$N'$	$N'' = 2$	$N'$	$N'' = 3$	$N'$	$N'' = 4$
0	$0.89727 \cdot 10^{-4}$	1	$0.89109 \cdot 10^{-4}$	2	$0.88827 \cdot 10^{-4}$	3	$0.88881 \cdot 10^{-4}$	4	$0.89283 \cdot 10^{-4}$
1	$0.90701 \cdot 10^{-4}$	2	$0.91056 \cdot 10^{-4}$	3	$0.91756 \cdot 10^{-4}$	4	$0.92812 \cdot 10^{-4}$	5	$0.94237 \cdot 10^{-4}$
2	$0.92672 \cdot 10^{-4}$	3	$0.94035 \cdot 10^{-4}$	4	$0.95771 \cdot 10^{-4}$	5	$0.97898 \cdot 10^{-4}$	6	$0.10044 \cdot 10^{-3}$
3	$0.95687 \cdot 10^{-4}$	4	$0.98117 \cdot 10^{-4}$	5	$0.10097 \cdot 10^{-3}$	6	$0.10426 \cdot 10^{-3}$	7	$0.10805 \cdot 10^{-3}$
$N'$	$N'' = 5$	$N'$	$N'' = 6$						
5	$0.90035 \cdot 10^{-4}$	6	$0.91153 \cdot 10^{-4}$						
6	$0.96050 \cdot 10^{-4}$	7	$0.98277 \cdot 10^{-4}$						
7	$0.10343 \cdot 10^{-3}$	8	$0.10690 \cdot 10^{-3}$						
8	$0.11235 \cdot 10^{-3}$	9	$0.11723 \cdot 10^{-3}$						

$\text{HCl}^+ \text{A } ^2\Sigma^+(v' = 8, N') \leftarrow \text{HCl}^+ \text{X } ^2\Pi_{3/2}(v'' = 0, N'')$									
$N'$	$N'' = 0$	$N'$	$N'' = 1$	$N'$	$N'' = 2$	$N'$	$N'' = 3$	$N'$	$N'' = 4$
0	$0.37884 \cdot 10^{-4}$	1	$0.37551 \cdot 10^{-4}$	2	$0.37368 \cdot 10^{-4}$	3	$0.37334 \cdot 10^{-4}$	4	$0.37452 \cdot 10^{-4}$
1	$0.38354 \cdot 10^{-4}$	2	$0.38492 \cdot 10^{-4}$	3	$0.38782 \cdot 10^{-4}$	4	$0.39233 \cdot 10^{-4}$	5	$0.39851 \cdot 10^{-4}$
2	$0.39309 \cdot 10^{-4}$	3	$0.39937 \cdot 10^{-4}$	4	$0.40735 \cdot 10^{-4}$	5	$0.41714 \cdot 10^{-4}$	6	$0.42889 \cdot 10^{-4}$
3	$0.40777 \cdot 10^{-4}$	4	$0.41932 \cdot 10^{-4}$	5	$0.43285 \cdot 10^{-4}$	6	$0.44854 \cdot 10^{-4}$	7	$0.46662 \cdot 10^{-4}$
$N'$	$N'' = 5$								
5	$0.37727 \cdot 10^{-4}$								
6	$0.40648 \cdot 10^{-4}$								
7	$0.44278 \cdot 10^{-4}$								
8	$0.48735 \cdot 10^{-4}$								

$\text{HCl}^+ \text{A } ^2\Sigma^+(v' = 9, N') \leftarrow \text{HCl}^+ \text{X } ^2\Pi_{3/2}(v'' = 0, N'')$									
$N'$	$N'' = 0$	$N'$	$N'' = 1$	$N'$	$N'' = 2$	$N'$	$N'' = 3$	$N'$	$N'' = 4$
0	$0.17096 \cdot 10^{-4}$	1	$0.16915 \cdot 10^{-4}$	2	$0.16796 \cdot 10^{-4}$	3	$0.16742 \cdot 10^{-4}$	4	$0.16751 \cdot 10^{-4}$
1	$0.17324 \cdot 10^{-4}$	2	$0.17370 \cdot 10^{-4}$	3	$0.17481 \cdot 10^{-4}$	4	$0.17660 \cdot 10^{-4}$	5	$0.17912 \cdot 10^{-4}$
2	$0.17788 \cdot 10^{-4}$	3	$0.18072 \cdot 10^{-4}$	4	$0.18431 \cdot 10^{-4}$	5	$0.18869 \cdot 10^{-4}$	6	$0.19395 \cdot 10^{-4}$
3	$0.18504 \cdot 10^{-4}$	4	$0.19047 \cdot 10^{-4}$	5	$0.19680 \cdot 10^{-4}$	6	$0.20413 \cdot 10^{-4}$	7	$0.21257 \cdot 10^{-4}$
$N'$	$N'' = 5$								
5	$0.16828 \cdot 10^{-4}$								
6	$0.18242 \cdot 10^{-4}$								
7	$0.20018 \cdot 10^{-4}$								
8	$0.22227 \cdot 10^{-4}$								

$\text{HCl}^+ \text{A } ^2\Sigma^+(v' = 10, N') \leftarrow \text{HCl}^+ \text{X } ^2\Pi_{3/2}(v'' = 0, N'')$									
$N'$	$N'' = 0$	$N'$	$N'' = 1$	$N'$	$N'' = 2$	$N'$	$N'' = 3$	$N'$	$N'' = 4$
0	$0.84832 \cdot 10^{-5}$	1	$0.83801 \cdot 10^{-5}$	2	$0.83035 \cdot 10^{-5}$	3	$0.82530 \cdot 10^{-5}$	4	$0.82286 \cdot 10^{-5}$
1	$0.85966 \cdot 10^{-5}$	2	$0.86062 \cdot 10^{-5}$	3	$0.86429 \cdot 10^{-5}$	4	$0.87077 \cdot 10^{-5}$	5	$0.88019 \cdot 10^{-5}$
2	$0.88276 \cdot 10^{-5}$	3	$0.89559 \cdot 10^{-5}$	4	$0.91154 \cdot 10^{-5}$	5	$0.93085 \cdot 10^{-5}$	6	$0.95382 \cdot 10^{-5}$
3	$0.91848 \cdot 10^{-5}$	4	$0.94427 \cdot 10^{-5}$	5	$0.97395 \cdot 10^{-5}$	6	$0.10080 \cdot 10^{-4}$	7	$0.10468 \cdot 10^{-4}$
$N'$	$N'' = 5$								
5	$0.82308 \cdot 10^{-5}$								
6	$0.89276 \cdot 10^{-5}$								
7	$0.98087 \cdot 10^{-5}$								
8	$0.10912 \cdot 10^{-4}$								

**Franck-Condon Faktoren für  $\text{DCI}^+ \text{A } ^2\Sigma^+ \leftarrow \text{DCI}^+ \text{X } ^2\Pi_{3/2}$ -Übergänge:**

<b><math>\text{DCI}^+ \text{A } ^2\Sigma^+(v' = 10, N') \leftarrow \text{DCI}^+ \text{X } ^2\Pi_{3/2}(v'' = 0, N'')</math></b>									
<b>N'</b>	<b>N'' = 0</b>	<b>N'</b>	<b>N'' = 1</b>	<b>N'</b>	<b>N'' = 2</b>	<b>N'</b>	<b>N'' = 3</b>	<b>N'</b>	<b>N'' = 4</b>
<b>0</b>	0.1880 $10^{-4}$	<b>1</b>	0.1870 $10^{-4}$	<b>2</b>	0.1862 $10^{-4}$	<b>3</b>	0.1857 $10^{-4}$	<b>4</b>	0.1855 $10^{-4}$
<b>1</b>	0.1893 $10^{-4}$	<b>2</b>	0.1894 $10^{-4}$	<b>3</b>	0.1899 $10^{-4}$	<b>4</b>	0.1906 $10^{-4}$	<b>5</b>	0.1916 $10^{-4}$
<b>2</b>	0.1917 $10^{-4}$	<b>3</b>	0.1931 $10^{-4}$	<b>4</b>	0.1948 $10^{-4}$	<b>5</b>	0.1969 $10^{-4}$	<b>6</b>	0.1992 $10^{-4}$
<b>3</b>	0.1955 $10^{-4}$	<b>4</b>	0.1982 $10^{-4}$	<b>5</b>	0.2012 $10^{-4}$	<b>6</b>	0.2046 $10^{-4}$	<b>7</b>	0.2084 $10^{-4}$

<b><math>\text{DCI}^+ \text{A } ^2\Sigma^+(v' = 11, N') \leftarrow \text{DCI}^+ \text{X } ^2\Pi_{3/2}(v'' = 0, N'')</math></b>									
<b>N'</b>	<b>N'' = 0</b>	<b>N'</b>	<b>N'' = 1</b>	<b>N'</b>	<b>N'' = 2</b>	<b>N'</b>	<b>N'' = 3</b>	<b>N'</b>	<b>N'' = 4</b>
<b>0</b>	0.1011 $10^{-4}$	<b>1</b>	0.1006 $10^{-4}$	<b>2</b>	0.1002 $10^{-4}$	<b>3</b>	0.1000 $10^{-4}$	<b>4</b>	0.9997 $10^{-5}$
<b>1</b>	0.1018 $10^{-4}$	<b>2</b>	0.1019 $10^{-4}$	<b>3</b>	0.1022 $10^{-4}$	<b>4</b>	0.1027 $10^{-4}$	<b>5</b>	0.1033 $10^{-4}$
<b>2</b>	0.1032 $10^{-4}$	<b>3</b>	0.1040 $10^{-4}$	<b>4</b>	0.1049 $10^{-4}$	<b>5</b>	0.1061 $10^{-4}$	<b>6</b>	0.1074 $10^{-4}$
<b>3</b>	0.1052 $10^{-4}$	<b>4</b>	0.1067 $10^{-4}$	<b>5</b>	0.1084 $10^{-4}$	<b>6</b>	0.1103 $10^{-4}$	<b>7</b>	0.1125 $10^{-4}$

<b><math>\text{DCI}^+ \text{A } ^2\Sigma^+(v' = 12, N') \leftarrow \text{DCI}^+ \text{X } ^2\Pi_{3/2}(v'' = 0, N'')</math></b>									
<b>N'</b>	<b>N'' = 0</b>	<b>N'</b>	<b>N'' = 1</b>	<b>N'</b>	<b>N'' = 2</b>	<b>N'</b>	<b>N'' = 3</b>	<b>N'</b>	<b>N'' = 4</b>
<b>0</b>	0.5635 $10^{-5}$	<b>1</b>	0.5610 $10^{-5}$	<b>2</b>	0.5598 $10^{-5}$	<b>3</b>	0.5601 $10^{-5}$	<b>4</b>	0.5616 $10^{-5}$
<b>1</b>	0.5675 $10^{-5}$	<b>2</b>	0.5690 $10^{-5}$	<b>3</b>	0.5719 $10^{-5}$	<b>4</b>	0.5762 $10^{-5}$	<b>5</b>	0.5817 $10^{-5}$
<b>2</b>	0.5757 $10^{-5}$	<b>3</b>	0.5813 $10^{-5}$	<b>4</b>	0.5883 $10^{-5}$	<b>5</b>	0.5968 $10^{-5}$	<b>6</b>	0.6066 $10^{-5}$
<b>3</b>	0.5881 $10^{-5}$	<b>4</b>	0.5980 $10^{-5}$	<b>5</b>	0.6094 $10^{-5}$	<b>6</b>	0.6223 $10^{-5}$	<b>7</b>	0.6367 $10^{-5}$

## 7.4 Abkürzungsverzeichnis

In der folgenden Tabelle sind die wichtigsten Abkürzungen und Symbole aufgeführt, die in dieser Arbeit verwendet werden:

<b>Symbol</b>	<b>Langschrift/Erklärung</b>
A	Spin-Bahn-Kopplungskonstante
AD	Spin-Bahn-Kopplungskonstante, höherer Term
AE	Auftrittsenergie
ASE	amplified spontaneous emission
B	Rotationskonstante
BBO	$\beta$ -Bariumborat ( $\beta$ -BaB <sub>2</sub> O <sub>4</sub> )
c	Lichtgeschwindigkeit
D	Zentrifugalaufweitungskonstante, quadratischer Term
D <sub>0</sub>	Dissoziationsenergie
e	Elementarladung
eV	Elektronenvolt
E	Energie
F(J)	Termenergie
FWHM	full width at half maximum
h	Plancksches Wirkungsquantum
H	Zentrifugalaufweitungskonstante, kubischer Term
$\Delta_f H^\circ$	Bildungswärme
IE	Ionisierungsenergie
I	Trägheitsmoment
I	Intensität
J	Gesamtdrehimpulsquantenzahl
n	Hauptquantenzahl
N	Rotationsquantenzahl
k	Kraftkonstante
k	Geschwindigkeitskonstante
KDP	Kaliumdihydrogenphosphat
l, L	Bahndrehimpulsquantenzahl
m	Masse
M	Multiplizität
MCP	micro channel plate
MPI	multiphoton ionization
Nd:YAG	Yttrium-Aluminium-Granat
P	Parität
PES	Photoelektronenspektroskopie
Q	Bahn-Rotations-Kopplungskonstante
QD	Bahn-Rotations-Kopplungskonstante, höherer Term
r	Kern-Kern-Abstand
R	Rydbergkonstante
<b>Symbol</b>	<b>Langschrift/Erklärung</b>

R	Übergangsmoment
REMPI	resonance enhanced multiphoton ionization
RLSF	rotational line strenght factor
s	Flugstrecke
s, S	Spindrehimpulsquantenzahl
$S_{(J,J)}$	Übergangsintensität
SHG	second harmonic generation
t	Flugzeit
T	Temperatur
THG	third harmonic generation
TOF	time of flight
U	Spannung
UV	ultraviolett
v	Geschwindigkeit
v	Schwingungsquantenzahl
$\delta$	Quantendefekt
$\gamma$	Spin-Rotations-Kopplungskonstante
$\lambda\gamma$	Wellenlänge
$\mu$	elektrisches Dipolmoment
$\mu$	reduzierte Masse
v	Frequenz
$\tilde{\nu}$	Wellenzahl
$\omega$	Winkelgeschwindigkeit
$\tau$	Lebensdauer
$\psi$	Wellenfunktion



## 7.5 Lebenslauf

Persönliche Daten	Michael Michel geb. Schumacher Hornstraße 19 10963 Berlin geb. am 27.02.1966 in Berlin geschieden, zwei Kinder
Schulbildung	1972 - 1974 Besuch der Elbe - Grundschule  1974 - 1976 Besuch der Adolf - Glaßbrenner - Grundschule  1976 - 1978 Besuch der Bürgermeister - Herz - Grundschule  1978 - 1984 Besuch des Leibniz - Gymnasiums, Dez. 1984 Abitur
Hochschulbildung	1985-1989 FU Berlin Studiengang Politologie  01.10.1989 FU Berlin Studiengang Chemie  24.05.1993 Vordiplom im Fach Chemie  17.12.1998 Diplom im Fach Chemie  01.01.1999 FU Berlin Promotionsstudium am ITPC
Erziehungsurlaub	Dez. 1993 – Dez. 1995